ÉCOLE POLYTECHNIQUE FÉDÉRALE DE LAUSANNE

MATHICSE

Mathematics Institute of Computational Science and Engineering

School of Basic Sciences - Section of Mathematics

MATHICSE Technical Report

Nr. 11.2015

Mai 2015

A model order reduction framework for parametrized nonlinear PDE constrained optimization

Federico Negri

http://mathicse.epfl.ch

Phone: +41 21 69 37648

Address:
EPFL - SB - MATHICSE (Bâtiment MA)
Station 8 - CH-1015 - Lausanne - Switzerland

Fax: +41 21 69 32545

A MODEL ORDER REDUCTION FRAMEWORK FOR PARAMETRIZED NONLINEAR PDE-CONSTRAINED OPTIMIZATION*

FEDERICO NEGRI†

Abstract. In this paper, we propose a model order reduction framework for parametrized quadratic optimization problems constrained by nonlinear stationary PDEs. Once the solutions of the optimization problem are characterized as the solutions of the corresponding optimality system, we build a reduced-order model following a suitable *all-at-once optimize-then-reduce* paradigm. Low-dimensional spaces for the state, control and adjoint variables are simultaneously constructed by means of either the Reduced Basis greedy algorithm or Proper Orthogonal Decomposition. In order to estimate the error between the high-fidelity and reduced solutions, we derive an a posteriori bound based on Brezzi-Rappaz-Raviart theory; further, a bound for the error on the cost functional is obtained. Then, for the sake of computational efficiency, we integrate into this framework the ROMES method presented in Drohmann et al. (2015) to generate tighter error indicators. Finally, this methodology is applied to the boundary optimal control of parametrized Navier-Stokes equations.

Key words. model order reduction, PDE-constrained optimization, reduced basis methods, a posteriori error estimates, Navier-Stokes equations, flow control.

AMS subject classifications. 35Q30, 49J20, 65K10, 65M15, 76D55

1. Introduction. The aim of this work is to propose a general approach for the construction of reduced-order models (ROMs) for parameterized PDE-constrained optimization problems of the following form: given $\boldsymbol{\mu} \in \mathcal{D}$,

$$(\mathbf{P}_{\boldsymbol{\mu}}) \qquad \min_{(y,u)\in Y\times\mathcal{U}} \mathcal{J}(y,u;\boldsymbol{\mu}) \quad \text{subject to} \quad \mathcal{E}(y,u;\boldsymbol{\mu}) = 0 \text{ in } Q'.$$

Here Y, $\mathcal{U}$, Q are Hilbert spaces along with their dual Y', $\mathcal{U}'$, Q', $y \in Y$ denotes the state variable, while $u \in \mathcal{U}$ is the control (or design) variable. The equality constraint $\mathcal{E}(\cdot;\cdot;\boldsymbol{\mu}) : Y \times \mathcal{U} \to Q'$ represents a (or a system of) stationary nonlinear PDE, while the cost functional $\mathcal{J}(\cdot,\cdot;\boldsymbol{\mu}) : Y \times \mathcal{U} \to \mathbb{R}$ is assumed to be quadratic. Both $\mathcal{J}$ and $\mathcal{E}$ may depend on a vector $\boldsymbol{\mu} \in \mathcal{D} \subset \mathbb{R}^P$ of $P \geq 1$ input parameters representing either physical or geometrical features.

After introducing a suitable full-order (or high-fidelity) discretization of the associated optimality system, solving the optimization problem $(\mathbf{P}_{\boldsymbol{\mu}})$ requires to solve a large scale system of nonlinear equations. To alleviate the computational burden, different model order reduction techniques have been developed to approximate $(\mathbf{P}_{\boldsymbol{\mu}})$ by projecting the full-order model (FOM) onto an appropriate subspace of much lower dimension spanned by a reduced-order basis. In particular, both Proper Orthogonal Decomposition (POD), see e.g. [38, 57, 30, 35, 54] and the recent survey [7], and the Reduced Basis (RB) method, see e.g. [17, 43, 45, 36, 44, 20, 37], have been successfully applied to a broad variety of optimization problems.

POD techniques have been originally used to deal with non-parametric time-dependent problems, see e.g. [4, 8, 30, 54], and then for parametric optimization problems [56, 3, 59], where parameters are considered as control variables. On the other hand, RB methods have been formerly developed to deal with parametric optimization problems, see e.g. [43, 56, 20]), and then parametrized (linear-quadratic)

*This work was supported by the Swiss National Science Foundation, project no. 141034.

†CMCS – Modelling and Scientific Computing, MATHICSE - Mathematics Institute of Computational Science and Engineering, EPFL, CH-1015 Lausanne, Switzerland (federico.negri@epfl.ch)

optimization problems [17, 45, 36, 44]. The latter refer to problems where the optimization is made with respect to some (either finite or infinite-dimensional) control variable u, rather than with respect to the parameters $\boldsymbol{\mu}$, which are instead treated as input data. This is the class of problems $(\mathbf{P}_{\boldsymbol{\mu}})$ belongs to.

In this context, the goal is to generate low-dimensional and fast, but still sufficiently accurate reduced-order models which are able to characterize the optimal solution of $(\mathbf{P}_{\boldsymbol{\mu}})$ for the whole range of input parameters we are interested in.

To this end, building upon the preliminary works [45, 44], we develop a reduction strategy based on a *all-at-once optimize-then-reduce* paradigm. Indeed, we characterize the solutions of the optimization problem as the solutions of the corresponding nonlinear system of optimality conditions. Then, we build – by means of either the RB greedy algorithm or POD – a reduced-order basis made of optimal state, adjoint and control snapshots. In particular, the reduction is operated on the state, control and adjoint variables simultaneously, by projecting the full-order optimality system onto the reduced basis. The resulting nonlinear, yet low-dimensional, set of equations is efficiently solved by means of a Newton-SQP method [33, 29] equipped with a suitable offline-online decomposition strategy.

Moreover, a residual-based a posteriori bound for the error between the full and reduced-order optimal solutions is obtained by applying Brezzi-Rappaz-Raviart theory [11, 12, 34, 58]. An offline-online decomposition strategy enabling a rapid evaluation of this bound is also developed. The numerical results show that the error bound correctly captures the error distribution over the parameter space. However, because of the severe ill-conditioning of this type of problems, it largely overestimates the error magnitude. Unfortunately, over-conservative error estimates lead to the construction of unnecessary large reduced spaces, thus affecting both the offline costs and the online efficiency.

To overcome this shortcoming, we resort to the ROM Error Surrogates (ROMES) method, recently proposed in [21]. The latter models the *bound-to-error map* as a Gaussian Process [50] and generates (at low cost) a much sharper estimate of the error. We then exploit this technique into usual POD and greedy strategies for the basis construction.

We specify this general framework in the case of boundary optimal control of the parametrized Navier-Stokes equations. The efficacy of the proposed method is demonstrated first on a two-dimensional Dirichlet boundary control problem modeling the optimization of an idealized arterial bypass graft, and then on a vorticity minimization problem for a parametrized bluff body immersed in a three-dimensional flow. In both cases, the optimal solutions exhibit a qualitatively different behavior as the parameters (affecting both the geometrical configuration and relevant physical properties such as the Reynolds number) vary. The ROM is able to correctly reproduce this variability by using just a small number of basis functions. As a result, significant speedups can be achieved, still ensuring a good accuracy.

The paper is organized as follows. In section 2 we introduce first and second order optimality conditions associated to problem $(\mathbf{P}_{\boldsymbol{\mu}})$; their full-order approximation is discussed in section 3. In section 5 we introduce the reduced-order approximation, its algebraic formulation and the offline-online computational strategy. A posteriori error estimates are derived in section 6, while the details about the construction of the reduced basis are given in section 8. Section 9 is devoted to the construction of a sharp error indicator using Gaussian Process regression. Numerical results are reported and discussed in sections 11 and 12. Finally, conclusions are offered in section 13.

2. First and second order optimality conditions. For our purposes, it is convenient to introduce the optimization variable $x = (y, u) \in X = Y \times \mathcal{U}$ and to express problem $(\mathbf{P}_{\boldsymbol{\mu}})$ in the so-called *full-space* formulation [29, 1]

$$\min_{x \in X} \ \mathcal{J}(x; \boldsymbol{\mu}) \quad \text{subject to} \quad \mathcal{E}(x; \boldsymbol{\mu}) = 0 \ \text{ in } Q'. \tag{2.1}$$

We thus treat the state and control variables as independent variables, linked by the constraint equation.

2.1. Lagrange multipliers and first order optimality conditions. Let us first define the Lagrangian functional $\mathcal{L}(x, p; \boldsymbol{\mu}) = \mathcal{J}(x; \boldsymbol{\mu}) + \langle \mathcal{E}(x; \boldsymbol{\mu}), p \rangle$, being $p \in Q$ a Lagrange multiplier associated to the constraint. For any fixed $\boldsymbol{\mu} \in \mathcal{D}$, we make the following assumptions [29, 33]:

- (H1) problem (2.1) has at least a local optimal solution $\bar{x} \in X$;
- (H2) the mappings $\mathcal{J}(\cdot; \boldsymbol{\mu}) \colon X \to \mathbb{R}$ and $\mathcal{E}(\cdot; \boldsymbol{\mu}) \colon X \to Q'$ are continuously Fréchet differentiable with Lipschitz continuous first derivatives $\mathcal{E}'(\cdot; \boldsymbol{\mu}) : X \to \mathcal{L}(X, Q')$ and $\mathcal{J}'(\cdot; \boldsymbol{\mu}) : X \to X'$, respectively;
- (H3) the Fréchet derivative of the state operator $\mathcal{E}'(\bar{x}; \boldsymbol{\mu})$ is surjective, i.e. there exists a constant $\bar{\lambda} > 0$ such that

$$\lambda(\boldsymbol{\mu}) = \inf_{\widehat{p} \in Q} \sup_{\widehat{x} \in X} \frac{\langle \mathcal{E}'(\bar{x}; \boldsymbol{\mu}) \widehat{x}, \widehat{p} \rangle}{\|\widehat{p}\|_Q \|\widehat{x}\|_X} > \bar{\lambda}. \tag{2.2}$$

Under these assumptions, for any given $\boldsymbol{\mu} \in \mathcal{D}$, if $\bar{x}$ is an optimal solution of (2.1) then there exists a Lagrange multiplier $\bar{p} \in Q$ such that $(\bar{x}, \bar{p})$ satisfies

$$\begin{cases} \mathcal{J}'(\bar{x}; \boldsymbol{\mu}) + \mathcal{E}'(\bar{x}; \boldsymbol{\mu})^* \bar{p} & = 0, \quad \text{in } X' \\ \mathcal{E}(\bar{x}; \boldsymbol{\mu}) & = 0, \quad \text{in } Q', \end{cases} \tag{2.3}$$

where $\mathcal{E}'(\bar{x}; \boldsymbol{\mu})^* \in \mathcal{L}(Q, X')$ denotes the adjoint of the Fréchet derivative of the state operator. The first order optimality system (2.3) can be also expressed in more compact form as

$$\mathcal{G}(U; \boldsymbol{\mu}) = \begin{pmatrix} \mathcal{J}'(x; \boldsymbol{\mu}) + \mathcal{E}'(x; \boldsymbol{\mu})^* p \\ \mathcal{E}(x; \boldsymbol{\mu}) \end{pmatrix} = 0 \qquad \text{in } \mathcal{X}', \tag{2.4}$$

being $U = (x, p) \in \mathcal{X}$, $\mathcal{X} = X \times Q$ and $\mathcal{G}(\cdot, \cdot; \boldsymbol{\mu}) : \mathcal{X} \to \mathcal{X}'$ defined as $\mathcal{G} = \nabla \mathcal{L}$.

2.2. Second order sufficient optimality condition. The optimality conditions (2.3) forms a nonlinear system of equations which represents the starting point to approximate the optimization problem (2.1). However, since a solution of (2.3) is not guaranteed to be a local minimizer of (2.1), we also require the following second order sufficient optimality condition:

- (H4) the mappings $\mathcal{J}(\cdot; \boldsymbol{\mu}) \colon X \to \mathbb{R}$ and $\mathcal{E}(\cdot; \boldsymbol{\mu}) \colon Y \to Q'$ are twice continuously Fréchet differentiable with Lipschitz continuous second derivatives and the operator $\mathcal{L}_{xx}(\bar{x}, \bar{p}; \boldsymbol{\mu})$ is coercive on the null space of $\mathcal{E}'(\bar{x}; \boldsymbol{\mu})$, i.e. there exists a constant $\bar{\alpha} > 0$ such that

$$\langle \mathcal{L}_{xx}(\bar{x}, \bar{p}; \boldsymbol{\mu}) d, d \rangle \geq \bar{\alpha} \|d\|_X^2, \qquad \forall d \in \ker \mathcal{E}'(\bar{x}; \boldsymbol{\mu}). \tag{2.5}$$

Under this condition, a solution $\bar{x}$ of (2.3) is a local minimizer of (2.1).

3. Full-order approximation. Let us first introduce suitable finite-dimensional approximation spaces $X_h \subset X$ and $Q_h \subset Q$. We then set $\mathcal{X}_h = X_h \times Q_h$ and denote with $N^h = N_x^h + N_p^h$ its dimension. Following a *discretize-then-optimize* approach, see e.g. [15, 26, 29], we consider the following full-order approximation of the optimization problem (2.1): given $\boldsymbol{\mu} \in \mathcal{D}$,

$$\min_{x_h \in X_h} \mathcal{J}_h(x_h; \boldsymbol{\mu}) \quad \text{subject to} \quad \langle \mathcal{E}_h(x_h; \boldsymbol{\mu}), \widehat{x} \rangle = 0 \quad \forall \widehat{x} \in X_h. \tag{3.1}$$

By requiring the gradient of the discrete Lagrangian $\mathcal{L}_h(x_h, p_h; \boldsymbol{\mu}) = \mathcal{J}_h(x_h; \boldsymbol{\mu}) + \langle \mathcal{E}_h(x_h; \boldsymbol{\mu}), p_h \rangle$ to vanish, we obtain the following optimality conditions

$$\mathcal{G}_h(U_h; \boldsymbol{\mu}) = \begin{pmatrix} \mathcal{J}_h'(x_h; \boldsymbol{\mu}) + \mathcal{E}_h'(x_h; \boldsymbol{\mu})^* p_h \\ \mathcal{E}_h(x_h; \boldsymbol{\mu}) \end{pmatrix} = 0 \qquad \text{in } \mathcal{X}_h'. \tag{3.2}$$

Upon defining the variational form

$$G(V; W; \boldsymbol{\mu}) =_{\mathcal{X}'} \langle \mathcal{G}_h(V; \boldsymbol{\mu}), W \rangle_{\mathcal{X}} \qquad \forall V, W \in \mathcal{X}_h,$$

problem (3.2) can be equivalently expressed in weak form: given $\boldsymbol{\mu} \in \mathcal{D}$, find $U_h(\boldsymbol{\mu}) \in \mathcal{X}_h$ such that

$$G(U_h; \widehat{U}; \boldsymbol{\mu}) = 0 \qquad \forall \widehat{U} \in \mathcal{X}_h. \tag{3.3}$$

For the well-posedness of the full-order approximation (3.3), it is sufficient to require the assumptions (H1)-(H4) to hold at the discrete level. In particular, denoting with $U_h = (x_h, p_h)$ a solution of (3.3), we require the derivative of the discretized state operator to be surjective, i.e.

$$\exists \bar{\lambda} > 0 \quad \text{s.t.} \quad \lambda_h(\boldsymbol{\mu}) = \inf_{\widehat{p} \in Q_h} \sup_{\widehat{x} \in X_h} \frac{\langle \mathcal{E}_h'(x_h; \boldsymbol{\mu}) \widehat{x}, \widehat{p} \rangle}{\|\widehat{p}\|_Q \|\widehat{x}\|_X} \geq \bar{\lambda}, \tag{3.4}$$

and the Hessian of the Lagrangian to satisfy a second order sufficient optimality condition

$$\exists \bar{\alpha}_h > 0 \quad \text{s.t.} \quad \langle \mathcal{L}_{h,xx}(x_h, p_h; \boldsymbol{\mu}) d, d \rangle \geq \bar{\alpha}_h \|d\|_X^2, \qquad \forall d \in X_h^0, \tag{3.5}$$

where $X_h^0 = \{ d \in X_h : \langle \mathcal{E}_h'(x_h; \boldsymbol{\mu}) d, \widehat{x} \rangle = 0, \, \forall \widehat{x} \in X_h \}$.

REMARK 4. *Conditions* (3.4)-(3.5) *are equivalent to the following*

$$\exists \bar{\beta} > 0 \quad \textit{s.t.} \quad \beta_h(U_h; \boldsymbol{\mu}) = \inf_{\widehat{U}_1 \in \mathcal{X}_h} \sup_{\widehat{U}_2 \in X_h} \frac{dG[U_h](\widehat{U}_1, \widehat{U}_2; \boldsymbol{\mu})}{\|\widehat{U}_1\|_{\mathcal{X}} \|\widehat{U}_2\|_{\mathcal{X}}} \geq \bar{\beta}, \tag{4.1}$$

where $dG[U_h](\cdot, \cdot; \boldsymbol{\mu}) : \mathcal{X} \times \mathcal{X} \to \mathbb{R}$ *denotes the Fréchet derivative of* $G(U_h; \cdot; \boldsymbol{\mu})$.

4.1. Newton method. The optimality conditions (3.2) form a finite-dimensional system of nonlinear equations. The Newton method applied to (2.4) reads: given $\boldsymbol{\mu} \in \mathcal{D}$ and an initial guess $U_h^0 \in \mathcal{X}_h$, for $k = 1, 2, \ldots$ until convergence, find $\delta U_h \in \mathcal{X}_h$ such that

$$\mathcal{G}_h'(U_h^k; \boldsymbol{\mu}) \, \delta U_h = -\mathcal{G}_h(U_h^k; \boldsymbol{\mu}) \quad \text{in } \mathcal{X}_h', \tag{4.2}$$

and then set $U_h^{k+1} = U_h^k + \delta U_h$. Here $\mathcal{G}_h'(V;\boldsymbol{\mu}) \in \mathcal{L}(\mathcal{X}_h;\mathcal{X}_h')$ denotes the Fréchet derivative of $\mathcal{G}_h$ at $V \in \mathcal{X}_h$. More in detail, the Newton step (4.2) reads: find $(\delta x_h^k, \delta p_h^k) \in X_h \times Q_h$ such that

$$\begin{pmatrix} \mathcal{L}_{h,xx}(x_h^k, p_h^k;\boldsymbol{\mu}) & \mathcal{E}_h'(x_h^k;\boldsymbol{\mu})^* \\ \mathcal{E}_h'(x_h^k;\boldsymbol{\mu}) & 0 \end{pmatrix} \begin{pmatrix} \delta x_h^k \\ \delta p_h^k \end{pmatrix} = - \begin{pmatrix} \mathcal{L}_{h,x}(x_h^k, p_h^k;\boldsymbol{\mu}) \\ \mathcal{E}_h(x_h^k;\boldsymbol{\mu}) \end{pmatrix}. \tag{4.3}$$

If the initial guess U_h^0 is sufficiently close to an optimal solution $\bar{U}_h$, assumptions (H1)-(H4) provide sufficient conditions for local quadratic convergence of Newton method, see e.g. [33].

The k-th step (4.2) can be equivalently formulated in weak form as: find $\delta U_h \in \mathcal{X}_h$ such that

$$dG[U_h^k](\delta U_h, \widehat{U};\boldsymbol{\mu}) = -G(U_h^k;\widehat{U};\boldsymbol{\mu}) \qquad \forall \widehat{U} \in \mathcal{X}_h. \tag{4.4}$$

4.2. Algebraic formulation. At the algebraic level, problem (3.3) leads to the following nonlinear system for $\mathbf{U}_h = (\mathbf{x}_h, \mathbf{p}_h) \in \mathbb{R}^{N^h}$

$$\mathbf{G}(\mathbf{U}_h;\boldsymbol{\mu}) = \begin{pmatrix} \mathbf{g}(\mathbf{x}_h;\boldsymbol{\mu}) + \mathrm{B}^T(\mathbf{x}_h;\boldsymbol{\mu})\,\mathbf{p}_h \\ \mathbf{E}(\mathbf{x}_h;\boldsymbol{\mu}) \end{pmatrix} = \mathbf{0}. \tag{4.5}$$

Here $\mathbf{g} \in \mathbb{R}^{N_p^h}$ is the discretized gradient of $\mathcal{J}_h$ with respect to x; $\mathbf{E} \in \mathbb{R}^{N_p^h}$ denotes the discretized constraint equation, while $\mathrm{B} \in \mathbb{R}^{N_p^h \times N_x^h}$ denotes its Jacobian with respect to the optimization variable. The k-th step of the Newton method applied to (4.5) can be written in compact algebraic form as follows: find $\delta\mathbf{U}_h \in \mathbb{R}^{N^h}$ such that

$$d\mathbf{G}(\mathbf{U}_h^k;\boldsymbol{\mu})\,\delta\mathbf{U}_h = -\mathbf{G}(\mathbf{U}_h^k;\boldsymbol{\mu}), \tag{4.6}$$

being $d\mathbf{G}(\cdot;\boldsymbol{\mu}) \in \mathbb{R}^{N^h \times N^h}$ the matrix resulting from the discretization of the Fréchet derivative $dG[\cdot](\cdot,\cdot;\boldsymbol{\mu})$. More in detail, (4.6) reads

$$\begin{pmatrix} \mathrm{H}(\mathbf{x}_h^k, \mathbf{p}_h^k;\boldsymbol{\mu}) & \mathrm{B}^T(\mathbf{x}_h^k;\boldsymbol{\mu}) \\ \mathrm{B}(\mathbf{x}_h^k;\boldsymbol{\mu}) & 0 \end{pmatrix} \begin{pmatrix} \delta\mathbf{x}_h \\ \delta\mathbf{p}_h \end{pmatrix} = - \begin{pmatrix} \mathbf{g}(\mathbf{x}_h^k;\boldsymbol{\mu}) + \mathrm{B}^T(\mathbf{x}_h^k;\boldsymbol{\mu})\mathbf{p}_h^k \\ \mathbf{E}(\mathbf{x}_h^k;\boldsymbol{\mu}) \end{pmatrix}, \tag{4.7}$$

where $\mathrm{H} \in \mathbb{R}^{N_x^h \times N_x^h}$ denotes the discretized Hessian of the Lagrangian with respect to x; $\delta\mathbf{x}_h \in \mathbb{R}^{N_x^h}$ and $\delta\mathbf{p}_h \in \mathbb{R}^{N_p^h}$ are the the search directions in the $\mathbf{x}$ and $\mathbf{p}$ variables, respectively.

5. Reduced-order approximation. The idea of reduced basis methods is to efficiently compute an approximate solution $x_N(\boldsymbol{\mu})$ of the full-order optimization problem (3.1) belonging to a low-dimensional space X_N generated by so called *snapshots*, i.e. solutions of the problem itself corresponding to suitably selected parameters. For the problem at hand, since the optimal solutions $x_h(\boldsymbol{\mu})$ of (3.1) are characterized as the solutions of the optimality system (3.3), two possible approaches to build a ROM can be pursued: the *reduce-then-optimize* and the *optimize-then-reduce* approach. Here we follow the second one, i.e. we build the ROM directly on the optimality system.

Let us denote with $X_N \subset X_h$ and $Q_N \subset Q_h$ suitably defined (see section 8) low-dimensional spaces generated by full-order snapshots of the optimization and adjoint variables, respectively. We then define the trial space $\mathcal{X}_N = X_N \times Q_N$ and we denote

by $\mathcal{W}_N \subset \mathcal{X}_h$ a suitable test space possibly different from $\mathcal{X}_N$. The Petrov-Galerkin reduced basis approximation of (3.3) reads: find $U_N(\boldsymbol{\mu}) \in \mathcal{X}_N$ such that

$$G(U_N; \widehat{U}; \boldsymbol{\mu}) = 0 \qquad \forall \widehat{U} \in \mathcal{W}_N. \tag{5.1}$$

The reduced optimality system (5.1) is a system of N nonlinear equations, which can be solved by means of Newton method. The generic k-th step reads: find $\delta U_N \in \mathcal{X}_N$ such that

$$dG[U_N^k](\delta U_N, \widehat{U}; \boldsymbol{\mu}) = -G(U_N^k; \widehat{U}; \boldsymbol{\mu}) \qquad \forall \widehat{U} \in \mathcal{W}_N. \tag{5.2}$$

The well-posedness of the reduced problem (5.1) as well as convergence of Newton method are ensured by Newton-Kantorovich theorem as long as the following inf-sup condition is fulfilled

$$\exists \bar{\beta} > 0 \quad \text{s.t.} \quad \beta_N(\boldsymbol{\mu}) = \inf_{V \in \mathcal{X}_N} \sup_{W \in \mathcal{W}_N} \frac{dG[U_N](V, W; \boldsymbol{\mu})}{\|V\|_{\mathcal{X}} \|W\|_{\mathcal{X}}} \geq \bar{\beta}. \tag{5.3}$$

The latter is equivalent to require assumptions (H3)-(H4) to hold at the reduced level. The fulfillment of these conditions has to be taken into account in the practical construction of the reduced spaces. Not only, we require the reduced spaces $\mathcal{X}_N, \mathcal{W}_N$ to provide (see [44] for a detailed discussion in the case of linear constraints):

- (A1) a *consistent approximation* of the optimality system, meaning that, if for some $\boldsymbol{\mu} \in \mathcal{D}$ we have $U_h(\boldsymbol{\mu}) \in \mathcal{X}_N$, then $U_N(\boldsymbol{\mu}) = U_h(\boldsymbol{\mu})$;
- (A2) a *Lagrangian preserving approximation*, so that (5.1) represents the gradient of the reduced Lagrangian functional $\mathcal{L}_N(\cdot, \cdot; \boldsymbol{\mu}) : X_N \times Q_N \to \mathbb{R}$ defined as

$$\mathcal{L}_N(v, q; \boldsymbol{\mu}) = \mathcal{L}_h(v, q; \boldsymbol{\mu}) \qquad \forall v \in X_N, q \in Q_N;$$

- (A3) a *stable approximation* in the sense of (5.3).

Since Galerkin projection automatically generates a ROM which enjoys property (A2) regardless of the definition of X_N and Q_N, we fix $\mathcal{W}_N = \mathcal{X}_N$.

5.1. Algebraic formulation. Let us denote by $\mathrm{V}_x \in \mathbb{R}^{N_x^h \times N_x}$ and $\mathrm{V}_p \in \mathbb{R}^{N_p^h \times N_p}$ suitable bases for the reduced spaces X_N and Q_N, respectively; a basis for $\mathcal{X}_N$ is therefore given by

$$\mathrm{V} = \begin{pmatrix} \mathrm{V}_x & 0 \\ 0 & \mathrm{V}_p \end{pmatrix} \in \mathbb{R}^{(N_x^h + N_p^h) \times (N_x + N_p)}.$$

Problem (5.1) is thus equivalent to the following nonlinear system of $N_x + N_p$ equations

$$\mathrm{V}^T \mathbf{G}(\mathrm{V}\mathbf{U}_N; \boldsymbol{\mu}) = \begin{pmatrix} \mathrm{V}_x^T \mathbf{g}(\mathrm{V}_x \mathbf{x}_N; \boldsymbol{\mu}) + \mathrm{V}_x^T \mathrm{B}^T(\mathrm{V}_x \mathbf{x}_N; \boldsymbol{\mu})\, \mathrm{V}_p \mathbf{p}_N \\ \mathrm{V}_p^T \mathbf{E}(\mathrm{V}_x \mathbf{x}_N; \boldsymbol{\mu}) \end{pmatrix} = \mathbf{0}, \tag{5.4}$$

where $\mathbf{x}_N$ and $\mathbf{p}_N$ denote the vectors of coefficients in the expansions of x_N and p_N with respect to the reduced bases. As already mentioned, thanks to the Galerkin projection, (5.4) represents the optimality system of the following reduced Lagrangian functional

$$\mathcal{L}_N(\mathbf{x}_N, \mathbf{p}_N; \boldsymbol{\mu}) = \mathcal{L}_h(\mathrm{V}_x \mathbf{x}_N, \mathrm{V}_p \mathbf{p}_N; \boldsymbol{\mu}) = \mathcal{J}_h(\mathrm{V}_x \mathbf{x}_N; \boldsymbol{\mu}) + \mathbf{p}_N^T \mathrm{V}_p^T \mathbf{E}(\mathrm{V}_x \mathbf{x}_N; \boldsymbol{\mu}). \tag{5.5}$$

The Newton step (5.2) is equivalent to the following linear system

$$d\mathbf{G}_N(\mathbf{U}_N^k;\boldsymbol{\mu})\,\delta\mathbf{U}_N = -\mathbf{G}_N(\mathbf{U}_N^k;\boldsymbol{\mu}), \tag{5.6}$$

where

$$d\mathbf{G}_N(\mathbf{U}_N^k;\boldsymbol{\mu}) = \mathrm{V}^T d\mathbf{G}(\mathrm{V}\mathbf{U}_N^k;\boldsymbol{\mu})\mathrm{V} = \begin{pmatrix} \mathrm{H}_N(\mathbf{x}_N^k,\mathbf{p}_N^k;\boldsymbol{\mu}) & \mathrm{B}_N^T(\mathbf{x}_N^k;\boldsymbol{\mu}) \\ \mathrm{B}_N(\mathbf{x}_N^k;\boldsymbol{\mu}) & 0 \end{pmatrix}, \tag{5.7}$$

$$\mathbf{G}_N(\mathbf{U}_N^k;\boldsymbol{\mu}) = \mathrm{V}^T\mathbf{G}(\mathrm{V}\mathbf{U}_N^k;\boldsymbol{\mu}) = \begin{pmatrix} \mathbf{g}_N(\mathbf{x}_N^k;\boldsymbol{\mu}) + \mathrm{B}_N^T(\mathbf{x}_N^k;\boldsymbol{\mu})\mathbf{p}_N^k \\ \mathbf{E}_N(\mathbf{x}_N^k;\boldsymbol{\mu}) \end{pmatrix}, \tag{5.8}$$

and the reduced matrices and vectors are given by:

$$\mathrm{H}_N(\mathbf{x}_N^k,\mathbf{p}_N^k;\boldsymbol{\mu}) = \mathrm{V}_x^T\,\mathrm{H}(\mathrm{V}_x\mathbf{x}_N^k,\mathrm{V}_p\mathbf{p}_N^k;\boldsymbol{\mu})\,\mathrm{V}_x, \qquad \mathrm{B}_N(\mathbf{x}_N^k;\boldsymbol{\mu}) = \mathrm{V}_p^T\,\mathrm{B}(\mathrm{V}_x\mathbf{x}_N^k;\boldsymbol{\mu})\,\mathrm{V}_x,$$
$$\mathbf{E}_N(\mathbf{x}_N^k;\boldsymbol{\mu}) = \mathrm{V}_p^T\,\mathbf{E}(\mathrm{V}_x\mathbf{x}_N^k;\boldsymbol{\mu}), \qquad \mathbf{g}_N(\mathbf{x}_N^k;\boldsymbol{\mu}) = \mathrm{V}_x^T\,\mathbf{g}(\mathrm{V}_x\mathbf{x}_N^k;\boldsymbol{\mu}).$$

5.2. Computational efficiency: offline-online decomposition. The (hopefully small) dimension $N \ll N_h$ of the linear system (5.6) to be solved at each Newton step does not warren subsantial computational savings, as the assembly of the reduced Jacobian matrix and residual vector still involves computations whose complexity depends on N^h. However, if the state equation features a low-order polynomial nonlinearity and the parametric dependence is affine, the assembly of the residual $\mathbf{G}_N(\cdot;\boldsymbol{\mu})$ and the matrix $d\mathbf{G}_N(\cdot;\boldsymbol{\mu})$ admits an efficient offline-online decomposition. For instance, in the case of quadratic nonlinearity (as for the Navier-Stokes equations, see Section 10) we can express the residual as

$$\mathbf{G}(\mathbf{W};\boldsymbol{\mu}) = \widetilde{\mathbf{G}}(\mathbf{W},\mathbf{W};\boldsymbol{\mu}),$$

$\widetilde{\mathbf{G}}(\cdot;\cdot;\boldsymbol{\mu})$ being linear w.r.t. the first two arguments. Then, thanks to the affine parametric dependence, we can assume the reduced residual to be expressed as

$$\mathbf{G}_N(\mathbf{W}_N;\boldsymbol{\mu}) = \sum_{q=1}^{Q_g} \theta_q^g(\boldsymbol{\mu}) \sum_{i,j=1}^{N} \mathbf{W}_{Ni}\mathbf{W}_{Nj}\,\mathrm{V}^T\widetilde{\mathbf{G}}_q(\boldsymbol{\phi}_i,\boldsymbol{\phi}_j), \tag{5.9}$$

for some suitable smooth functions $\theta_q^g : \mathcal{D} \to \mathbb{R}$ and $\boldsymbol{\mu}$-independent vectors $\widetilde{\mathbf{G}}_q(\cdot,\cdot) \in \mathbb{R}^{N^h}$ (denoting by $\boldsymbol{\phi}_i$ the elements of the basis V). Similarly, we can express the Jacobian matrix as

$$d\mathbf{G}_N(\mathbf{W}_N;\boldsymbol{\mu}) = \sum_{q=1}^{Q_d} \theta_q^d(\boldsymbol{\mu}) \sum_{i=1}^{N} \mathbf{W}_{Ni}\,\mathrm{V}^T d\mathbf{G}_q(\boldsymbol{\phi}_i)\mathrm{V}, \tag{5.10}$$

for suitable smooth functions $\theta_q^d : \mathcal{D} \to \mathbb{R}$ and $\boldsymbol{\mu}$-independent matrices $d\mathbf{G}_q(\boldsymbol{\phi}_n) \in \mathbb{R}^{N^h \times N^h}$. The NQ_d reduced matrices $\mathrm{V}^T d\mathbf{G}_q(\boldsymbol{\phi}_i)\mathrm{V}$ and the N^2Q_g vectors $\mathrm{V}^T\widetilde{\mathbf{G}}_q(\boldsymbol{\phi}_i,\boldsymbol{\phi}_j)$ can be precomputed offline, so that online the reduced problem can be assembled and solved with complexity independent of N^h.

On the other hand, if the problem features a higher (or nonpolynomial) nonlinearity and possibly a nonaffine parametric dependence, we must introduce a further level

of reduction – called hyper-reduction or system approximation [13] – by suitably employing techniques such as EIM [5, 22], DEIM [14] or gappy POD [13] to approximate the nonlinear/nonaffine terms and recover an affine structure. All these approaches are aimed at obtaining an affine approximation of the residual of the form

$$\mathbf{G}(\mathbf{W}_N;\boldsymbol{\mu}) \approx \sum_{m=1}^{M} \alpha_m^g(\boldsymbol{\mu};\mathbf{W}_N)\,\mathbf{G}_m. \tag{5.11}$$

being $\{\mathbf{G}_m\}_{m=1}^M$ a basis for a suitable subspace of $\mathcal{M}_{\mathbf{G}} = \{\mathbf{G}(\mathrm{V}\mathbf{U}_N(\boldsymbol{\mu});\boldsymbol{\mu}) : \boldsymbol{\mu}\in\mathcal{D}\}$ and $\alpha_m^g(\cdot;\cdot)$ some interpolation coefficients to be determined[1].

6. A posteriori error estimates. In order to derive an a posteriori error estimate for the error on the state, control and adjoint variables, we take advantage of Brezzi-Rappaz-Raviart theory [11, 12], as applied originally in [34, 58] to the reduced basis approximation of the Navier-Stokes equations.

We start by introducing all the involved quantities. First,

$$\epsilon_N(\boldsymbol{\mu}) = \|G(U_N;\cdot;\boldsymbol{\mu})\|_{\mathcal{X}_h'} = \sup_{W\in\mathcal{X}_h} \frac{G(U_N;W;\boldsymbol{\mu})}{\|W\|_{\mathcal{X}}} \tag{6.1}$$

is the dual norm of the residual of the optimality system (5.1). Next, we need the inf-sup constant $\beta_h^N(\boldsymbol{\mu})$ of the Fréchet derivative dG at U_N

$$\beta_h^N(\boldsymbol{\mu}) = \inf_{V\in\mathcal{X}_h}\sup_{W\in\mathcal{X}_h} \frac{dG[U_N(\boldsymbol{\mu})](V,W;\boldsymbol{\mu})}{\|V\|_{\mathcal{X}}\|W\|_{\mathcal{X}}}, \tag{6.2}$$

and an upper bound $K_h^N(\boldsymbol{\mu})$ for its Lipschitz constant[2] such that, for all $V\in\overline{B}\big(U_N(\boldsymbol{\mu}), 2\epsilon_N(\boldsymbol{\mu})/\beta_h^N(\boldsymbol{\mu})\big)$

$$\|dG[U_N(\boldsymbol{\mu})](\cdot,\cdot;\boldsymbol{\mu}) - dG[V](\cdot,\cdot;\boldsymbol{\mu})\|_{\mathcal{L}(\mathcal{X}_h,\mathcal{X}_h')} \le K_h^N(\boldsymbol{\mu})\|U_N(\boldsymbol{\mu}) - V\|_{\mathcal{X}}. \tag{6.3}$$

Here $\overline{B}(x,\alpha)\subset\mathcal{X}_h$ denotes a closed ball with center x and radius α. Finally, we define the *proximity indicator*

$$\tau_N(\boldsymbol{\mu}) = \frac{4K_h^N(\boldsymbol{\mu})\epsilon_N(\boldsymbol{\mu})}{\big(\beta_h^N(\boldsymbol{\mu})\big)^2}. \tag{6.4}$$

A straightforward application of [12, Theorem 2.1] (see also [34, 58]) provides the following bound for the norm of the error $E_N(\boldsymbol{\mu}) = U_h(\boldsymbol{\mu}) - U_N(\boldsymbol{\mu})$.

PROPOSITION 6.1. *If $\tau_N(\boldsymbol{\mu}) < 1$, then there exists a unique solution $U_h(\boldsymbol{\mu}) \in B\big(U_N(\boldsymbol{\mu}), 2\epsilon_N(\boldsymbol{\mu})/\beta_h^N(\boldsymbol{\mu})\big)$ of (3.3). Moreover,*

$$\|E_N(\boldsymbol{\mu})\|_{\mathcal{X}} \le \Delta_N(\boldsymbol{\mu}) := \frac{2}{2-\tau_N(\boldsymbol{\mu})}\,\frac{\epsilon_N(\boldsymbol{\mu})}{\beta_h^N(\boldsymbol{\mu})}. \tag{6.5}$$

[1] Note that (5.9) can be written in this form with $M = Q_g N^2$, $\mathbf{G}_m = \widetilde{\mathbf{G}}_q(\boldsymbol{\phi}_j,\boldsymbol{\phi}_j)$ and $\alpha_m^g(\boldsymbol{\mu};\mathbf{W}_N) = \theta_q^g(\boldsymbol{\mu})\mathbf{W}_{Ni}\mathbf{W}_{Nj}$.

[2] The Lipschitz continuity of dG follows from assumption (H2).

6.1. Error estimate on the cost functional. In order to obtain a bound for the error on the cost functional, we combine the error bound (6.5) with some results from goal-oriented a posteriori error analysis. Let us first define the following estimator

$$\Delta_N^{\mathcal{J}} = \frac{1}{2}\Delta_N(\boldsymbol{\mu})\,\epsilon_N(\boldsymbol{\mu}).$$

PROPOSITION 6.2. *For the reduced basis approximation* (5.1) *of the full-order problem* (3.3) *with nonlinear state equation and quadratic cost functional, if* $\tau_N(\boldsymbol{\mu}) < 1$ *there holds*

$$|\mathcal{J}_h(x_h;\boldsymbol{\mu}) - \mathcal{J}_h(x_N;\boldsymbol{\mu})| \leq \Delta_N^{\mathcal{J}}(\boldsymbol{\mu}) + |\mathcal{R}(E_N(\boldsymbol{\mu});\boldsymbol{\mu})|, \tag{6.6}$$

where the remainder term $\mathcal{R}(E_N(\boldsymbol{\mu});\boldsymbol{\mu})$ *can be estimated by*

$$|\mathcal{R}(E_N(\boldsymbol{\mu});\boldsymbol{\mu})| \leq \sup_{W\in[U_N,U_h]} |d^2G[W](E_N(\boldsymbol{\mu}),E_N(\boldsymbol{\mu}),E_N(\boldsymbol{\mu});\boldsymbol{\mu})|. \tag{6.7}$$

Proof. We adapt here the result proved in [6, Prop. 6.1]. If the ROM (5.1) preserves the Lagrangian structure (assumption A2), we have that $\mathcal{J}_h(x_h;\boldsymbol{\mu}) - \mathcal{J}_h(x_N;\boldsymbol{\mu}) = \mathcal{L}_h(U_h;\boldsymbol{\mu}) - \mathcal{L}_h(U_N;\boldsymbol{\mu})$. By applying the mean value theorem we then obtain,

$$\mathcal{L}_h(U_h;\boldsymbol{\mu}) - \mathcal{L}_h(U_N;\boldsymbol{\mu}) = \int_0^1 \nabla\mathcal{L}_h(U_h + s(U_N - U_h);\boldsymbol{\mu})(E_N)\,ds.$$

Approximating the integral with the trapezoidal rule and by the problem statement (3.3) we get,

$$\mathcal{L}_h(U_h;\boldsymbol{\mu}) - \mathcal{L}_h(U_N;\boldsymbol{\mu}) = \tfrac{1}{2}\nabla\mathcal{L}_h(U_N;\boldsymbol{\mu})(E_N) + \mathcal{R}(E_N(\boldsymbol{\mu});\boldsymbol{\mu}),$$

where the remainder term $\mathcal{R}$ is given by

$$\mathcal{R}(E_N;\boldsymbol{\mu}) = -\tfrac{1}{12}\nabla_h^3\mathcal{L}(\hat{W};\boldsymbol{\mu})(E_N,E_N,E_N;\boldsymbol{\mu}) = -\tfrac{1}{12}d^2G[\hat{W}](E_N,E_N,E_N;\boldsymbol{\mu}),$$

for some $\hat{W}$ lying between U_h and U_N. Then, since $\nabla\mathcal{L}_h(U_N;\boldsymbol{\mu})(E_N) = G(U_N;E_N);\boldsymbol{\mu})$, if $\tau_N(\boldsymbol{\mu}) < 1$ we can bound the first term as,

$$|\nabla\mathcal{L}_h(U_N;\boldsymbol{\mu})(E_N)| = |G(U_N;E_N);\boldsymbol{\mu})| \leq \epsilon_N(\boldsymbol{\mu})\|E_N(\boldsymbol{\mu})\|_{\mathcal{X}} \leq \epsilon_N(\boldsymbol{\mu})\Delta_N(\boldsymbol{\mu}),$$

which yields (6.6). ∎

REMARK 7. *If the state equation is linear, we recover the error estimates obtained in [45] by means of Babuška stability theory:*

$$\|E_N(\boldsymbol{\mu})\|_{\mathcal{X}} \leq \Delta_N^L(\boldsymbol{\mu}) := \frac{\epsilon_N(\boldsymbol{\mu})}{\beta_h(\boldsymbol{\mu})}, \qquad |\mathcal{J}_h(x_h;\boldsymbol{\mu}) - \mathcal{J}_h(x_N;\boldsymbol{\mu})| \leq \frac{1}{2}\Delta_N^L(\boldsymbol{\mu})\epsilon_N(\boldsymbol{\mu}),$$

since $\Delta_N(\boldsymbol{\mu}) \equiv \Delta_N^L(\boldsymbol{\mu})$ *and the remainder term is identically zero. Moreover, in the nonlinear case, if the ROM is consistent,* $\epsilon_N(\boldsymbol{\mu})$ *tends to zero as* N *increases and therefore also* $\tau_N(\boldsymbol{\mu})$ *tends to zero, so that the nonlinear error estimator* $\Delta_N(\boldsymbol{\mu})$ *reduces to* $\Delta_N^L(\boldsymbol{\mu})$*. The latter can thus be conveniently used as error indicator in place of* $\Delta_N(\boldsymbol{\mu})$*.*

7.1. Efficient evaluation of the error estimate. The error estimates (6.5)-(6.6) admit the usual efficient offline-online decomposition [51], that we briefly summarize here. We start by evaluating the dual norm of the residual $\epsilon_N(\boldsymbol{\mu})$ efficiently, thanks to the affine decomposition (5.11):

$$\epsilon_N(\boldsymbol{\mu})^2 = \|\mathbf{G}(\mathrm{V}\mathbf{U}_N;\boldsymbol{\mu})\|^2_{\mathrm{X}^{-1}} = \sum_{m_1,m_2=1}^{M} \underbrace{\alpha^g_{m_1}(\boldsymbol{\mu};\mathbf{U}_N)\,\alpha^g_{m_2}(\boldsymbol{\mu};\mathbf{U}_N)}_{\text{online}}\ \underbrace{\mathbf{G}^T_{m_1}\mathrm{X}^{-1}\mathbf{G}_{m_2}}_{\text{offline}},$$

$\mathrm{X} \in \mathbb{R}^{N_h \times N_h}$ being a matrix realizing the $\mathcal{X}_h$-norm.

The second step involves the evaluation of the stability factor $\beta_h^N(\boldsymbol{\mu})$, for which we provide the heuristic approximation proposed in [41]. As $\beta_h^N(\boldsymbol{\mu})$ converges to $\beta_h(\boldsymbol{\mu})$ as $U_N(\boldsymbol{\mu})$ approaches $U_h(\boldsymbol{\mu})$, the latter quantity represents a N-independent surrogate for $\beta_h^N(\boldsymbol{\mu})$. Then, $\beta_h(\boldsymbol{\mu})$ is approximated by an interpolant $\beta_I(\boldsymbol{\mu})$ obtained through an adaptive *Radial Basis Functions* interpolation procedure. As a result, $\beta_h^N(\boldsymbol{\mu})$ is approximated by a surrogate $\beta_I(\boldsymbol{\mu})$ whose online evaluation has a computational complexity independent of the dimension N^h. For the details of this procedure we refer to [41].

Finally, we have to provide an upper bound $K_h^N(\cdot;\boldsymbol{\mu})$ to the Lipshitz constant of dG, which however depends on the problem at hand. We shall see an example dealing with the optimal control of Navier-Stokes equations in Section 10.

7.2. Error estimate for the control variable. An alternative bound for the error in the control variable can be obtained by considering the following (equivalent) reduced-space formulation of the optimization problem (3.1):

$$\min_{u_h \in \mathcal{U}_h} \widehat{\mathcal{J}}_h(u_h;\boldsymbol{\mu}) := \mathcal{J}_h(y_h(u_h;\boldsymbol{\mu}),u_h;\boldsymbol{\mu}), \tag{7.1}$$

where we have denoted by $u_h \mapsto y_h(u_h;\boldsymbol{\mu})$ the solution operator of $\mathcal{E}_h(y_h,u_h;\boldsymbol{\mu}) = 0$.

The first order optimality condition for the unconstrained optimization problem (7.1) reads: given $\boldsymbol{\mu} \in \mathcal{D}$, find $u_h \in \mathcal{U}_h$ such that

$$\widehat{\mathcal{J}}'_h(u_h;\boldsymbol{\mu}) = 0 \quad \text{in } \mathcal{U}'_h. \tag{7.2}$$

The first derivative of $\widehat{\mathcal{J}}_h$ is given by

$$\widehat{\mathcal{J}}'_h(u_h;\boldsymbol{\mu}) = \mathcal{E}_{h,u}(y_h,u_h;\boldsymbol{\mu})^* p_h + \mathcal{J}_{h,u}(y_h,u_h;\boldsymbol{\mu}),$$

where $y_h = y_h(u_h;\boldsymbol{\mu})$, and $p_h = p_h(u_h;\boldsymbol{\mu})$ satisfies the adjoint equation

$$\mathcal{E}_{h,y}(y_h,u_h;\boldsymbol{\mu})^* p_h = -\mathcal{J}_{h,y}(y_h,u_h;\boldsymbol{\mu}).$$

By applying Brezzi-Rappaz-Raviart theory (or equivalently Newton-Kantorovich theorem, see e.g. [60]) to the nonlinear problem (7.2) we obtain the following bound[3]

$$\|u_h(\boldsymbol{\mu}) - u_N(\boldsymbol{\mu})\|_{\mathcal{U}} \le \frac{2}{\lambda_h^N(\boldsymbol{\mu})} \|\widehat{\mathcal{J}}'_h(u_N(\boldsymbol{\mu});\boldsymbol{\mu})\|_{\mathcal{U}'}, \tag{7.3}$$

where

$$\lambda_h^N(\boldsymbol{\mu}) = \inf_{v \in \mathcal{U}_h} \frac{\langle \widehat{\mathcal{J}}''_h(u_N(\boldsymbol{\mu});\boldsymbol{\mu})v, v\rangle}{\|v\|^2_{\mathcal{U}}}$$

[3]More rigorously, the bound only holds if $u_N(\boldsymbol{\mu})$ satisfies a *proximity condition* similar to the one of Proposition 6.1.

is the coercivity constant of the Hessian $\widehat{\mathcal{J}}_h''$. For any $v_h \in \mathcal{U}_h$, the latter is given by [29, 33]

$$\widehat{\mathcal{J}}_h''(v_h;\boldsymbol{\mu}) = T_h(v_h;\boldsymbol{\mu})^* \; \mathcal{L}_{h,xx}(y_h(v_h;\boldsymbol{\mu}), v_h, p(v_h;\boldsymbol{\mu});\boldsymbol{\mu}) \; T_h(v_h;\boldsymbol{\mu}).$$

with

$$T_h(v_h;\boldsymbol{\mu}) = \begin{pmatrix} -\mathcal{E}_{h,y}(y_h(v_h;\boldsymbol{\mu}), v_h)^{-1}\mathcal{E}_{h,u}(y_h(v_h;\boldsymbol{\mu}), v_h) \\ I_{\mathcal{U}_h} \end{pmatrix} \in \mathcal{L}(\mathcal{U}_h, Y_h \times \mathcal{U}_h)$$

and $I_{\mathcal{U}_h} : \mathcal{U}_h \to \mathcal{U}_h$ the identity operator.

The error bound (7.3) was already obtained in different forms in [57, 35, 36, 20, 44]. However, since $\widehat{\mathcal{J}}_h'(u_N(\boldsymbol{\mu});\boldsymbol{\mu})$ is an implicit operator, we cannot set up a straightforward offline-online strategy for the computation of its norm. For this reason, in the following we rather rely on the *full-space* estimates (6.5)-(6.6).

8. Reduced bases construction. For the practical construction of the reduced space $\mathcal{X}_N$, different strategies can be employed. The first option is to rely on the well-known greedy algorithm [49, 51] guided by the a posteriori error estimate (6.5). At each iteration N, we select the parameter $\boldsymbol{\mu}^{N+1}$ which maximizes $\Delta_N(\boldsymbol{\mu})$ over a training set $\Xi_{\text{train}} \subset \mathcal{D}$, and then enrich the current basis V using $\mathbf{U}_h(\boldsymbol{\mu}^N)$. The algorithm stops when a desired accuracy (or a maximum number of iterations) is reached. The procedure requires to solve only N full-order optimization problems; however the update (at each iteration) of the ingredients required to evaluate the dual norm of the residual can highly affect the offline costs (both in terms of computational time and memory storage), especially for large N, Q_d, Q_g.

An alternative approach relies on Proper Orthogonal Decomposition, see e.g. [53, 31]. First, a set of N_s snapshots $\{\mathbf{U}_h(\boldsymbol{\mu}^n)\}_{n=1}^{N_s}$ is computed for some configurations $\boldsymbol{\mu}^n \in \mathcal{D}$ (selected either a priori guided by physical intuition or by sampling techniques like latin hypercube sampling (LHS) or sparse grids). Then, the basis V is constructed by retaining the first N left singular vectors in the singular value decomposition of the snapshot matrix $S = [\mathbf{U}_h(\boldsymbol{\mu}^1) \cdots \mathbf{U}_h(\boldsymbol{\mu}^{N_s})]$. With respect to the previous option, here we usually have to solve a higher number ($N_s > N$) of full-order optimization problems. However, since the error estimate in this case only serves for the online certification, its ingredients are assembled only once and for all after the ROM construction. Then, the error estimate can be evaluated over a test sample $\Xi_{\text{test}} \subset \mathcal{D}$ to check whether the maximum (or average) error is below a desired tolerance. If not, the POD basis can be suitably enriched by either including some of the discarded singular vectors or computing new snapshots.

The choice between these two strategies is influenced by several factors: besides the dimension N^h of the problem, the number of affine terms Q_g and Q_d and the dimension of the parameter space $\mathcal{D}$, also the software implementation and the available computational resources play an important role. However, in both cases the availability of a tight error estimate is crucial to (i) avoid oversampling in the offline phase and (ii) effectively quantify the accuracy of the reduced approximation in the online phase. We further address these aspects in the next section.

9. Tight error indicator by Gaussian Process regression. The sharpness of the error estimator $\Delta_N(\boldsymbol{\mu})$ is measured by the effectivity factor

$$\eta_N(\boldsymbol{\mu}) = \frac{\Delta_N(\boldsymbol{\mu})}{\|E_N(\boldsymbol{\mu})\|_{\mathcal{X}}}.$$

PROPOSITION 9.1. *If $\tau_N(\boldsymbol{\mu}) < 1$, we have the following bounds on the effectivity factor*

$$1 \leq \eta_N(\boldsymbol{\mu}) \leq 4\frac{\gamma_h^N(\boldsymbol{\mu})}{\beta_h^N(\boldsymbol{\mu})}, \tag{9.1}$$

where $\gamma_h^N(\boldsymbol{\mu})$ denotes the continuity constant of the Fréchet derivative dG at $U_N(\boldsymbol{\mu})$.

Proof. The lower bound directly follows from Proposition 6.1. We now prove the upper bound (omitting the $\boldsymbol{\mu}$-dependence for clarity). Using equations (3.3), (5.1) and the mean value theorem, we have for all $V \in \mathcal{X}_h$

$$\begin{aligned} G(U_N; V) = &-dG[U_N](U_h - U_N, V) \\ &+ \int_0^1 [dG[U_N](U_h - U_N, V) - dG[U_N + s(U_h - U_N)](U_h - U_N, V)]\, ds. \end{aligned}$$

Then, since $U_h \in B(U_N, 2\epsilon_N/\beta_h^N)$ and $\tau_N < 1$,

$$\epsilon_N \leq \gamma_h^N \|E_N\|_{\mathcal{X}} + \frac{K_h^N}{2}\|E_N\|_{\mathcal{X}}^2 \leq \gamma_h^N \|E_N\|_{\mathcal{X}} + \frac{1}{2}\epsilon_N,$$

whence $\epsilon_N \leq 2\gamma_h^N \|E_N\|_{\mathcal{X}}$. Thus,

$$\Delta_N = \frac{2}{2 - \tau_N}\,\frac{\epsilon_N}{\beta_h^N} \leq 4\frac{\gamma_h^N}{\beta_h^N}\|E_N\|_{\mathcal{X}},$$

which proves the second inequality in (9.1). ∎

The upper bound of the estimate (9.1) is closely related to the condition number $\kappa_h(\boldsymbol{\mu}) = \gamma_h(\boldsymbol{\mu})/\beta_h(\boldsymbol{\mu})$ of the Hessian dG. Since PDE-constrained optimization problems are known to be often severely ill-conditioned (see, e.g., [1] and references therein), we cannot expect the error estimator $\Delta_N(\boldsymbol{\mu})$ to be sufficiently tight. However, as already mentioned, over-conservative error estimates lead to the construction of unnecessary large reduced spaces, thus affecting both the offline costs and the online efficiency.

To overcome this shortcoming, we resort to the ROM Error Surrogates (ROMES) method proposed in [21] (see also [47, 42]). The key assumption, that will be numerically verified in Sections 11 and 12, is that both $\Delta_N(\boldsymbol{\mu})$ and $\Delta_N^L(\boldsymbol{\mu})$ strongly correlate with $\|E_N(\boldsymbol{\mu})\|_{\mathcal{X}}$. Exploiting this property, the ROMES method allows to generate a tight estimate $\widehat{\Delta}_N(\boldsymbol{\mu})$ of the error by approximating the one-dimensional map $\Delta_N^L(\boldsymbol{\mu}) \mapsto \|E_N(\boldsymbol{\mu})\|_{\mathcal{X}}$ using Gaussian Process (GP) regression [50]. We briefly summarize here how to construct such an estimator, referring to [21] for further details.

For the time being, we assume to have a set $\mathcal{T}_N$ of $M_r \geq 2$ training points

$$\mathcal{T}_N = \left\{ \left(\Delta_n^L(\boldsymbol{\mu}^{i_n}), \|E_n(\boldsymbol{\mu}^{i_n})\|_{\mathcal{X}}\right) : \{(n, \boldsymbol{\mu}^{i_n})\} \subseteq \{1, \ldots, N\} \times \mathcal{D} \right\} \subset \mathbb{R}^2, \tag{9.2}$$

obtained by evaluating the error and its estimate for different parameter values and dimensions of the ROM; we will discuss later how to generate this training set. Based on $\mathcal{T}_N$, we construct by means of Gaussian Process (GP) regression [50] a statistical model of the unknown deterministic error $\|E_N(\boldsymbol{\mu})\|_{\mathcal{X}}$ as a function of $\Delta_N^L(\boldsymbol{\mu})$. To this

end, let us denote by $d = \log \Delta_N^L$ the independent variable and by $f = \log \|E_N\|_{\mathcal{X}}$ the dependent one. Moreover we define a vector of training points $\mathbf{d} \in \mathbb{R}^{M_r}$ and a vector $\mathbf{f} \in \mathbb{R}^{M_r}$ of training targets as

$$\mathbf{d}_i = \log(r_i), \qquad \mathbf{f}_i = \log(s_i), \qquad (r_i, s_i) \in \mathcal{T}_N, \ i = 1, \dots, M_r.$$

Using these training data, for any given test point $d_* \in \mathbb{R}$, the GP method generates a predictive Gaussian distribution

$$f_* | \mathbf{d}, \mathbf{f}, d_* \sim \mathcal{N}(\nu(d_*), \bar{\sigma}(d_*)) \tag{9.3}$$

with mean $\nu(d_*)$ and covariance $\bar{\sigma}(d_*)$. These latter are given by

$$\nu(d_*) = \mathbf{k}_*^T (\mathrm{K} + \sigma_{M_r}^2 \mathrm{I})^{-1} \mathbf{f}, \qquad \bar{\sigma}(d_*) = \mathrm{K} - \mathbf{k}_*^T (\mathrm{K} + \sigma_{M_r}^2 \mathrm{I})^{-1} \mathbf{k}_*,$$

where the matrix $\mathrm{K} \in \mathbb{R}^{M_r \times M_r}$ and the vector $\mathbf{k}_* \in \mathbb{R}^{M_r}$ are defined as

$$\mathrm{K}_{ij} = k(\mathbf{d}_i, \mathbf{d}_j), \qquad \mathbf{k}_i = k(\mathbf{d}_i, d_*), \qquad k(x, y) = \sigma^2 \exp\left(-\frac{|x-y|^2}{2l^2}\right).$$

The free parameters $(l, \sigma, \sigma_{M_r})$ are determined as the maximizers of the log-likelihood function (see e.g. [50])

$$g(l, \sigma, \sigma_{M_r}) = \tfrac{1}{2} \mathbf{f}^T (\mathrm{K}(l, \sigma) + \sigma_{M_r}^2 \mathrm{I})^{-1} \mathbf{f} - \tfrac{1}{2} \log |\mathrm{K}(l, \sigma) + \sigma_{M_r}^2 \mathrm{I}| - \tfrac{M_r}{2} \log(2\pi).$$

We can now define a *probabilistic upper bound* $f_*^+ : \mathbb{R} \to \mathbb{R}$ of the unknown error as the $100(1-\alpha)\%$ upper predictive interval of the GP regression model

$$f_*^+(d_*) = \nu(d_*) + \sqrt{2}\, \mathrm{erf}^{-1}(1-\alpha)\ \bar{\sigma}(d_*).$$

This latter implicitly defines the error indicator $\widehat{\Delta}_N : \mathcal{D} \to \mathbb{R}^+$,

$$\widehat{\Delta}_N(\boldsymbol{\mu}) = \exp\Big(\nu(\log \Delta_N^L(\boldsymbol{\mu})) + \sqrt{2}\, \mathrm{erf}^{-1}(1-\alpha)\ \bar{\sigma}(\log \Delta_N^L(\boldsymbol{\mu}))\Big). \tag{9.4}$$

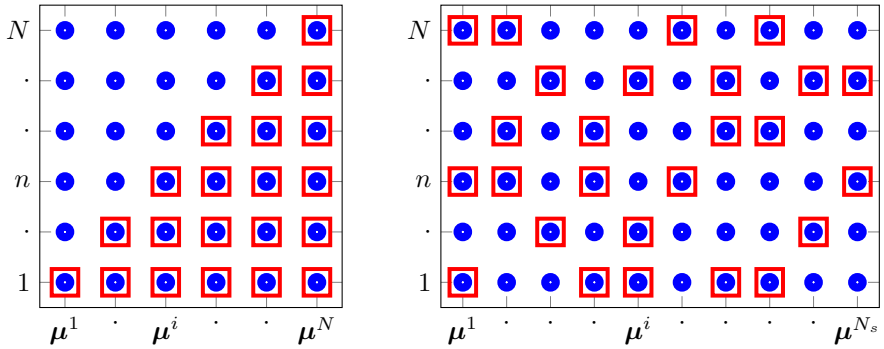

FIG. 9.1. *Scheme for the construction of the regression data set $\mathcal{T}_N$ when the using greedy algorithm (left) and POD (right). The blue circles represent the points where the exact error $\|E_n(\boldsymbol{\mu}^i)\|_{\mathcal{X}}$ is available, while red squares represent those used to build $\mathcal{T}_N$.*

The training set $\mathcal{T}_N$ is constructed in a different way depending on the strategy used to build the ROM. In the case the greedy algorithm is used, at the generic iteration N we have N^2 candidate training points $(\Delta_n^L(\boldsymbol{\mu}^n), \|E_n(\boldsymbol{\mu}^n)\|)$, $1 \le n \le N$,

where both the estimate and the exact error are available.[4] However, thanks to assumption (A1), $\|E_n(\boldsymbol{\mu}^i)\|_{\mathcal{X}} \approx 0$ for $n \geq i$. On one hand, the points where the error vanishes are not as important as the ones corresponding to unexplored regions of the parameter space; on the other hand, discarding all these points from the training set would yield a very poor estimator in these (untrained) regions. We thus propose to discard the points corresponding to the first $n-1$ training inputs of the ROM of dimension n, so that $\mathcal{T}_N$ is only made of the following $M_r = N(N+1)/2$ points (see also Fig. 9.1)

$$\mathcal{T}_N = \Big\{ \big(\Delta_n^L(\boldsymbol{\mu}^i),\, \|E_n(\boldsymbol{\mu}^i)\|_{\mathcal{X}}\big), \quad n = 1, \dots, i, \quad i = 1, \dots, N \Big\}. \tag{9.5}$$

The GP regression model is then embedded in the usual greedy procedure [49, 51] as described in Algorithm 1.

Input: Maximum number of iterations $N_{\max}$, stopping tolerance $\epsilon_g > 0$, training sample $\Xi_{\text{train}} \subset \mathcal{D}$, starting point $\boldsymbol{\mu}^1 \in \mathcal{D}$

$N = 0$, $\delta_0 = \epsilon_g + 1$, $\mathrm{V} = \emptyset$, $\mathcal{T}_0 = \emptyset$
while $N < N_{\max}$ and $\delta_N > \epsilon_g$ **do**
  $N \leftarrow N + 1$
  compute $\mathbf{U}_h(\boldsymbol{\mu}^N)$ by solving the FOM (4.5)
  update reduced basis $\mathrm{V} \leftarrow \mathrm{V} \cup \mathbf{U}_h(\boldsymbol{\mu}^N)$
  set $\mathcal{T}_N = \mathcal{T}_{N-1}$
  for $n = 1 : N$ **do**
    $\mathcal{T}_N \leftarrow \mathcal{T}_N \cup \big(\Delta_n^L(\boldsymbol{\mu}^N), \|E_n(\boldsymbol{\mu}^N)\|_{\mathcal{X}}\big)$
  end for
  if $N \geq 2$
    build surrogate error model and associated upper bound $\widehat{\Delta}_N(\boldsymbol{\mu})$
  else
    $\widehat{\Delta}_N(\boldsymbol{\mu}) = \Delta_N(\boldsymbol{\mu})$
  end if
  $[\delta_N, \boldsymbol{\mu}^{N+1}] = \max_{\boldsymbol{\mu} \in \Xi_{\text{train}}} \widehat{\Delta}_N(\boldsymbol{\mu})$
end while

Algorithm 1: Greedy algorithm guided by the error indicator $\widehat{\Delta}_N(\boldsymbol{\mu})$.

If a POD approach is used, the regression model is built only once and for all after the snapshots collection and the construction of the ROM. In this case, there are $N_s N$ candidate training points where computing the exact error and its estimate is relatively cheap. In fact, already for a moderate number of snapshots and basis functions, say $N_s \approx 100$ and $N \approx 20$, generating the entire training set $\mathcal{T}_N$ and the corresponding regression model can be quite time-consuming. Therefore, we define $\mathcal{T}_N$ as a random subset of the available $N_s N$ points (see also Fig. 9.1)

$$\mathcal{T}_N \subseteq \Big\{ \big(\Delta_n^L(\boldsymbol{\mu}^i),\, \|E_n(\boldsymbol{\mu}^i)\|_{\mathcal{X}}\big), \quad n = 1, \dots, N, \quad i = 1, \dots, N_s \Big\}. \tag{9.6}$$

10. Dirichlet boundary control of the Navier-Stokes equations. As a notable instance of problems which fit into this framework, we consider the following

[4] Given a ROM of dimension N, all the ROMs of dimension $n = 1, \dots, N-1$ are readily available as long as the reduced spaces are hierarchical. This is the case when using both greedy and POD procedures.

parametrized boundary control problem [32, 24, 27]: find a triple $(\mathbf{v}, \pi, \mathbf{u})$ such that the cost functional

$$\mathcal{J}(\mathbf{v}, \pi, \mathbf{u}; \boldsymbol{\mu}) = \mathcal{F}_1(\mathbf{v}; \boldsymbol{\mu}) + \mathcal{F}_2(\mathbf{u}; \boldsymbol{\mu}) \tag{10.1}$$

is minimized subject to the steady Navier-Stokes equations

$$\begin{aligned} -\nu\Delta\mathbf{v} + (\mathbf{v}\cdot\nabla)\mathbf{v} + \nabla\pi &= \mathbf{0} \qquad && \text{in } \Omega(\boldsymbol{\mu}) \\ \nabla\cdot\mathbf{v} &= 0 && \text{in } \Omega(\boldsymbol{\mu}), \end{aligned} \tag{10.2}$$

with boundary conditions

$$\begin{aligned} \mathbf{v} &= \mathbf{u} && \text{on } \Gamma_C(\boldsymbol{\mu}) \\ \mathbf{v} &= \mathbf{0} && \text{on } \Gamma_w(\boldsymbol{\mu}) \\ -\pi\mathbf{n} + \nu(\nabla\mathbf{v})\mathbf{n} &= \mathbf{0} && \text{on } \Gamma_N(\boldsymbol{\mu}). \end{aligned} \tag{10.3}$$

Here $\Omega(\boldsymbol{\mu}) \subset \mathbb{R}^d$ $(d = 2, 3)$ is a parametrized spatial domain with Lipschitz boundary $\partial\Omega = \Gamma_C \cup \Gamma_N \cup \Gamma_w$, being $\Gamma_D = \Gamma_C \cup \Gamma_w$ the Dirichlet portion of the boundary and Γ_N the Neumann one; the state variables $\mathbf{v}$ and π denote the velocity and pressure fields, respectively, while $\mathbf{u}$ acts as a Dirichlet boundary control. In the cost functional $\mathcal{J}$, $\mathcal{F}_1(\mathbf{v}; \boldsymbol{\mu})$ represents the objective to be minimized, while $\mathcal{F}_2(\mathbf{u}; \boldsymbol{\mu})$ is a regularization term ensuring the coercivity of the functional. Possible choices for $\mathcal{F}$ are the viscous energy dissipation, vorticity or velocity tracking type functionals [28].

In view of the application presented in Section 11, we also consider an additional constraint on the control variable, described by a bounded linear functional $l(\cdot; \boldsymbol{\mu}) \in U'$

$$l(\mathbf{u}; \boldsymbol{\mu}) = C(\boldsymbol{\mu}) \qquad \forall \mathbf{u} \in U, \tag{10.4}$$

$C(\boldsymbol{\mu}) \in \mathbb{R}$ being a given function of the parameters. The constraint (10.4) can be used for instance to impose a desired flux on the control boundary Γ_C.

10.1. Weak formulation. In order to cast the optimal control problem (10.1)-(10.3) in the general formulation $(\mathbf{P}_{\boldsymbol{\mu}})$-(2.1), we first define the velocity space V

$$V = \mathbf{H}^1_D(\Omega) := \Big\{ \mathbf{v} \in [H^1(\Omega)]^d \colon \mathbf{v} = 0 \text{ on } \Gamma_D \Big\},$$

the pressure space $M = L^2(\Omega)$, and the state space $Y = V \times M$. While the natural choice for the control space would be $\mathcal{U} = \mathbf{H}^{1/2}(\Gamma_C) = [H^{1/2}(\Gamma_C)]^d$, we rather assume higher regularity by defining $\mathcal{U} = \mathbf{H}^1(\Gamma_C)$ ($\mathcal{U} = \mathbf{H}^1_0(\Gamma_C)$ if Γ_C has a boundary), in order to avoid the involved calculation of the $\mathbf{H}^{1/2}(\Gamma_C)$-inner product. To account for the Dirichlet control, we split the velocity field as $\mathbf{v} = \mathbf{v}_0 + \mathbf{R}(\mathbf{u})$, where $\mathbf{v}_0 \in \mathbf{H}^1_D(\Omega)$, $\mathbf{R} \colon \mathcal{U} \to \mathbf{H}^1_w(\Omega)$ is a bounded extension operator such that $\mathbf{R}(\mathbf{u}) \in \mathbf{H}^1_w(\Omega)$ and $\mathbf{R}(\mathbf{u})|_{\Gamma_C} = \mathbf{u}$. For the sake of simplicity, we still denote $\mathbf{v}_0$ with $\mathbf{v}$, as no ambiguity occurs.

We define the following bilinear and trilinear forms associated with the differential operators:

$$a(\mathbf{v}, \widehat{\boldsymbol{\lambda}}; \boldsymbol{\mu}) := \int_{\Omega(\boldsymbol{\mu})} \nabla\mathbf{v} \cdot \nabla\widehat{\boldsymbol{\lambda}}\, d\Omega, \quad b(\mathbf{v}, \widehat{\eta}; \boldsymbol{\mu}) := -\int_{\Omega(\boldsymbol{\mu})} \widehat{\eta}\nabla\cdot\mathbf{v}\, d\Omega, \quad \forall\, \mathbf{v}, \widehat{\boldsymbol{\lambda}} \in V,\ \widehat{\eta} \in M,$$

$$c(\mathbf{v}_1, \mathbf{v}_2, \widehat{\boldsymbol{\lambda}}; \boldsymbol{\mu}) := \int_{\Omega(\boldsymbol{\mu})} (\mathbf{v}_1\cdot\nabla)\mathbf{v}_2 \cdot \widehat{\boldsymbol{\lambda}}\, d\Omega, \qquad \forall\, \mathbf{v}_1, \mathbf{v}_2, \widehat{\boldsymbol{\lambda}} \in V,$$

$$d(\mathbf{v}_1, \mathbf{v}_2, \widehat{\boldsymbol{\lambda}}; \boldsymbol{\mu}) := c(\mathbf{v}_1, \mathbf{v}_2, \widehat{\boldsymbol{\lambda}}; \boldsymbol{\mu}) + c(\mathbf{v}_2, \mathbf{v}_1, \widehat{\boldsymbol{\lambda}}; \boldsymbol{\mu}), \qquad \forall\, \mathbf{v}_1, \mathbf{v}_2, \widehat{\boldsymbol{\lambda}}, \in V,$$

and a compound bilinear form $S(\cdot,\cdot;\boldsymbol{\mu})\colon Y\times Y\to\mathbb{R}$ representing the Stokes operator

$$S(\mathbf{v},\pi;\boldsymbol{\lambda},\eta;\boldsymbol{\mu}) = a(\mathbf{v},\boldsymbol{\lambda};\boldsymbol{\mu}) + b(\boldsymbol{\lambda},\pi;\boldsymbol{\mu}) + b(\mathbf{v},\eta;\boldsymbol{\mu}). \tag{10.5}$$

Since the Navier-Stokes equations can be considered with values in $\widetilde{Q}' = Y'$, we set $\widetilde{Q} = Y$ and define the operator $\mathcal{E}_1(\cdot;\boldsymbol{\mu})\colon X\to\widetilde{Q}'$ as

$${}_{\widetilde{Q}'}\langle\mathcal{E}_1(x;\boldsymbol{\mu}),\widehat{p}\rangle_{\widetilde{Q}} = S(\mathbf{v}+\mathbf{R}(\mathbf{u}),\pi;\widehat{\boldsymbol{\lambda}},\widehat{\eta};\boldsymbol{\mu}) + c(\mathbf{v}+\mathbf{R}(\mathbf{u}),\mathbf{v}+\mathbf{R}(\mathbf{u}),\widehat{\boldsymbol{\lambda}};\boldsymbol{\mu}). \tag{10.6}$$

Then, we define the operator $\mathcal{E}_2(\cdot;\boldsymbol{\mu})\colon\mathcal{U}\to\mathbb{R}$ as $\mathcal{E}_2(x;\boldsymbol{\mu}) = l(\mathbf{u};\boldsymbol{\mu}) - C(\boldsymbol{\mu})$. This fits the abstract formulation (2.1), upon defining the operator $\mathcal{E}(\cdot;\boldsymbol{\mu}) : X\to Q'$, with $Q = \widetilde{Q}\times\mathbb{R}$, as

$$\mathcal{E}(x;\boldsymbol{\mu}) = \begin{pmatrix}\mathcal{E}_1(x;\boldsymbol{\mu})\\ \mathcal{E}_2(x;\boldsymbol{\mu})\end{pmatrix}. \tag{10.7}$$

Finally, let us express the quadratic functionals $\mathcal{F}_1$ and $\mathcal{F}_2$ appearing in (10.1) as

$$\mathcal{F}_1(\mathbf{v};\boldsymbol{\mu}) = \frac{1}{2}m(\mathbf{v},\mathbf{v};\boldsymbol{\mu}) \qquad \mathcal{F}_2(\mathbf{u};\boldsymbol{\mu}) = \frac{\sigma}{2}n(\mathbf{u},\mathbf{u};\boldsymbol{\mu}),$$

where $m(\cdot,\cdot;\boldsymbol{\mu})\colon\ Z\times Z\to\mathbb{R}$ is a symmetric, continuous, non-negative bilinear form over an Hilber space $Z\supset V$, $\sigma>0$ is a given constant, while $n(\cdot,\cdot;\boldsymbol{\mu})\colon\mathcal{U}\times\mathcal{U}\to\mathbb{R}$ is a symmetric, bounded and coercive bilinear form.

From the existence of solutions of the steady Navier-Stokes equations (10.2) (under the assumption of *small data*), see e.g. [25, 55], and the properties of $\mathcal{J}$, it follows by standard arguments (see e.g. [19, 27, 28]) that for each $\boldsymbol{\mu}\in\mathcal{D}$ there exists at least one optimal solution $\bar{x}\in X$.

10.2. Optimality conditions. Let us introduce the Lagrange functional[5] $\mathcal{L}(\cdot;\boldsymbol{\mu}) : X\times Q_1\times\mathbb{R}\to\mathbb{R}$,

$$\mathcal{L}(x,p,\kappa;\boldsymbol{\mu}) = \mathcal{J}(x;\boldsymbol{\mu}) + \langle p,\mathcal{E}_1(x;\boldsymbol{\mu})\rangle + \kappa\,\mathcal{E}_2(x;\boldsymbol{\mu}). \tag{10.8}$$

In order to ensure the existence of Lagrange multipliers associated to an optimal solution $\bar{x}$, we have to verify the fulfillment of assumptions (H2) and (H3). As regards the former, we start by computing the Fréchet derivatives of $\mathcal{E}_1$ at $x\in X$ in directions $\delta x,\delta^2 x\in X$ (we omit the $\boldsymbol{\mu}$-dependence of the variational forms for clarity):

$$\langle\mathcal{E}_1'(x;\boldsymbol{\mu})\delta x,p\rangle = S(\delta\mathbf{v}+\mathbf{R}(\delta\mathbf{u}),\delta\pi;\boldsymbol{\lambda},\eta) + d(\delta\mathbf{v}+\mathbf{R}(\delta\mathbf{u}),\mathbf{v}+\mathbf{R}(\mathbf{u}),\boldsymbol{\lambda}),\quad\forall p\in\widetilde{Q},$$
$$\langle\mathcal{E}_1''(x;\boldsymbol{\mu})(\delta x,\delta^2 x),p\rangle = d(\delta\mathbf{v}+\mathbf{R}(\delta\mathbf{u}),\delta^2\mathbf{v}+\mathbf{R}(\delta^2\mathbf{u}),\boldsymbol{\lambda}),\quad\forall p\in\widetilde{Q}.$$

As the nonlinearities are quadratic, all higher derivatives are identically equal to zero. For the linear constraint $\mathcal{E}_2$, it holds

$$\mathcal{E}_2'(x;\boldsymbol{\mu})\delta x = l(\delta\mathbf{u};\boldsymbol{\mu}),\qquad \mathcal{E}_2''(x;\boldsymbol{\mu})(\delta x,\delta^2 x) = 0.$$

Therefore, $\mathcal{E}$ is twice continuously differentiable and its second derivative is Lipschitz continuous since it does not depend on $x\in X$. The first and second derivatives of $\mathcal{J}$ at $x\in X$ are given by

$$\mathcal{J}'(x;\boldsymbol{\mu})\delta x = m(\mathbf{v}+\mathbf{R}(\mathbf{u}),\delta\mathbf{v}+\mathbf{R}(\delta\mathbf{u});\boldsymbol{\mu}) + \sigma n(\mathbf{u},\delta\mathbf{u};\boldsymbol{\mu}), \tag{10.9}$$

$$\mathcal{J}''(x;\boldsymbol{\mu})(\delta x,\delta^2 x) = m(\delta^2\mathbf{v}+\mathbf{R}(\delta^2\mathbf{u}),\delta\mathbf{v}+\mathbf{R}(\delta\mathbf{u});\boldsymbol{\mu}) + \sigma n(\delta^2\mathbf{u},\delta\mathbf{u};\boldsymbol{\mu}), \tag{10.10}$$

[5]Here we denote with p the Lagrange multiplier associated to $\mathcal{E}_1$ rather than $\mathcal{E}$ as in the previous sections, as no ambiguity occurs.

so that also $\mathcal{J}$ satisfy assumption (H2). Finally, assumption (H3), i.e. the surjectivity of the linearization of the constraint $\mathcal{E}$, can be proved by following the arguments in [27, 28]. We end up with the following

PROPOSITION 10.1. *Suppose that, for a given $\boldsymbol{\mu} \in \mathcal{D}$, $\bar{x} \in X$ is a local solution to* (10.1)-(10.2)*. Then there exist unique Lagrange multipliers $\bar{p} \in \widetilde{Q}, \bar{\kappa} \in \mathbb{R}$ such that $(\bar{x}, \bar{p}, \bar{\kappa})$ satisfy*

$$\begin{cases} \mathcal{J}'(\bar{x};\boldsymbol{\mu}) + \mathcal{E}_1'(\bar{x};\boldsymbol{\mu})^* \bar{p} + \mathcal{E}_2'(\bar{x};\boldsymbol{\mu})^* \bar{\kappa} & = 0, \quad \text{in } X' \\ \mathcal{E}_1(\bar{x};\boldsymbol{\mu}) & = 0, \quad \text{in } Q' \\ \mathcal{E}_2(\bar{x};\boldsymbol{\mu}) & = 0, \quad \text{in } \mathbb{R}. \end{cases} \tag{10.11}$$

This means that, given $\boldsymbol{\mu} \in \mathcal{D}$, solving the optimization problem (10.1)-(10.3) *requires to find $(\mathbf{v}, \pi; \mathbf{u}; \boldsymbol{\lambda}, \eta; \kappa) \in Y \times \mathcal{U} \times \widetilde{Q} \times \mathbb{R}$ such that*

$$\begin{cases} S(\widehat{\mathbf{v}}, \widehat{\pi}; \boldsymbol{\lambda}, \eta) + d(\widehat{\mathbf{v}}, \mathbf{v} + \mathbf{R}(\mathbf{u}), \boldsymbol{\lambda}) = -m(\mathbf{v} + \mathbf{R}(\mathbf{u}), \widehat{\mathbf{v}}), & \forall (\widehat{\mathbf{v}}, \widehat{\pi}) \in Y \\ \sigma n(u, \widehat{u}) + d(\mathbf{R}(\widehat{u}), \mathbf{v} + \mathbf{R}(\mathbf{u}), \boldsymbol{\lambda}) + m(\mathbf{v} + \mathbf{R}(\mathbf{u}), \mathbf{R}(\widehat{u})) \\ \qquad = -\kappa l(\widehat{u};\boldsymbol{\mu}) - S(\mathbf{R}(\widehat{u}), 0; \boldsymbol{\lambda}, \eta), & \forall \widehat{u} \in \mathcal{U} \\ S(\mathbf{v} + \mathbf{R}(\mathbf{u}), \pi; \widehat{\boldsymbol{\lambda}}, \widehat{\eta}) + c(\mathbf{v} + \mathbf{R}(\mathbf{u}), \mathbf{v} + \mathbf{R}(\mathbf{u}), \widehat{\boldsymbol{\lambda}}) = 0, & \forall (\widehat{\boldsymbol{\lambda}}, \eta) \in \widetilde{Q} \\ l(\mathbf{u};\boldsymbol{\mu}) = C(\boldsymbol{\mu}). \end{cases} \tag{10.12}$$

For the proof of the coercivity of the Lagrangian (necessary for the fulfillment of condition (H4)) we refer to [19, 28] and references therein. We simply report the expression of the Hessian of the Lagrangian at $x \in X$ in the direction $\delta x \in X$

$$\begin{aligned} \langle \mathcal{L}_{xx}(x, p; \boldsymbol{\mu}) \delta x, \delta x \rangle = \mathcal{J}''(x;\boldsymbol{\mu})(\delta x, \delta x) + \langle \mathcal{E}_1''(x;\boldsymbol{\mu})(\delta x, \delta^2 x), p \rangle = \sigma n(\delta \mathbf{u}, \delta \mathbf{u}; \boldsymbol{\mu}) \\ + m(\delta \mathbf{v} + \mathbf{R}(\delta \mathbf{u}), \delta \mathbf{v} + \mathbf{R}(\delta \mathbf{u}); \boldsymbol{\mu}) + d(\delta \mathbf{v} + \mathbf{R}(\delta \mathbf{u}), \delta \mathbf{v} + \mathbf{R}(\delta \mathbf{u}), \boldsymbol{\lambda}; \boldsymbol{\mu}). \end{aligned}$$

10.3. Full-order discretization. For the full-order approximation of (10.1)-(10.3), we use $\mathbb{P}^1$-$\mathbb{P}^1$ finite element spaces with Dohrmann-Bochev stabilization [10] to approximate velocity and pressure variables, as well as $\mathbb{P}^1$ finite elements to discretize the control variable. Note that since the pressure stabilization is symmetric, optimize-then-discretize and discretize-then-optimize approaches commute in this case.

Moreover, for the numerical experiments discussed in the following sections, a continuation strategy with respect to Reynolds number (see e.g. [32, 9]) demonstrates to be sufficient to globalize Newton method, without resorting to suitable line search or trust region algorithms.

10.4. Reduced spaces definition. In order to build reduced spaces satisfying assumptions (A1)-(A3), we employ a slightly modified version of the aggregated strategy proposed in [44]: we use aggregated pressure and velocity spaces for the state and adjoint variables as in [44], but without enriching the velocity space by supremizer solutions. Indeed, in all our numerical experiments the pressure stabilization demonstrates to guarantee the solvability of the state operator also at the reduced level, without the need of enriching the velocity space.

We first describe the construction using the greedy algorithm. We denote by $S_N = \{\boldsymbol{\mu}^1, \ldots, \boldsymbol{\mu}^N\}$ the parameter samples selected by the greedy algorithm and consider the corresponding (suitably orthonormalized) full-order solutions $(x_h(\boldsymbol{\mu}^n)$,

$p_h(\boldsymbol{\mu}^n))$, $1 \le n \le N$. We define the aggregated pressure and velocity spaces M_N, V_N as

$$M_N = \text{span}\big\{\pi_h(\boldsymbol{\mu}^n),\, \eta_h(\boldsymbol{\mu}^n)\big\}_{n=1}^N, \qquad V_N = \text{span}\big\{\mathbf{v}_h(\boldsymbol{\mu}^n), \boldsymbol{\lambda}_h(\boldsymbol{\mu}^n)\big\}_{n=1}^N.$$

Then, we define the reduced space $\mathcal{U}_N = \text{span}\{\mathbf{u}_h(\boldsymbol{\mu}^n)\}_{n=1}^N$ for the control variable.

If a POD approach is used instead, we first compute full-order solutions $(x_h(\boldsymbol{\mu}_i)$, $p_h(\boldsymbol{\mu}_i))$, $i = 1, \cdots, N_s$ of the optimality system for N_s parameters value $\boldsymbol{\mu}_i$ chosen by LHS sampling. Then, we perform POD separately on each variable in order to obtain (i) the reduced state velocity and pressure spaces V_N^s, M_N^s; (ii) the reduced adjoint velocity and pressure spaces V_N^a, M_N^a; (iii) the reduced control space $\mathcal{U}_N$. Finally, we define the aggregated spaces as:

$$M_N = M_N^s \cup M_N^a, \qquad V_N = V_N^s \cup V_N^a.$$

In both cases, we finally set

$$Y_N = V_N \times M_N, \qquad X_N = Y_N \times \mathcal{U}_N, \qquad \widetilde{Q}_N = Y_N, \qquad \mathcal{X}_N = X_N \times \widetilde{Q}_N \times \mathbb{R},$$

so that the reduced space $\mathcal{X}_N$ has dimension $9N + 1$.

10.5. Error estimates. Let us denote by $\rho_h = \rho_h(\Omega)$ the *discrete* $L^4(\Omega)$-$H^1(\Omega)$ Sobolev embedding constant [40]; moreover we denote by V_h a suitable finite element subspace for V. Then, the continuity of the trilinear form $c(\cdot,\cdot,\cdot;\boldsymbol{\mu})$ yields

$$c(\mathbf{v}_1, \mathbf{v}_2, \boldsymbol{\lambda}; \boldsymbol{\mu}) \le \rho_h^2 M_c(\boldsymbol{\mu}) \|\mathbf{v}_1\|_V \|\mathbf{v}_2\|_V \|\boldsymbol{\lambda}\|_V, \qquad \forall \mathbf{v}_1, \mathbf{v}_2, \boldsymbol{\lambda} \in V_h,$$

where $M_c(\boldsymbol{\mu})$ is a function depending on the parametrization (see [40] for further details).

PROPOSITION 10.2. *The Lipschitz constant of the Fréchet derivative* $dG[\cdot](\cdot,\cdot;\boldsymbol{\mu})$ *associated to problem* (10.1)-(10.2) *is bounded by the positive function*

$$K_h^N(\boldsymbol{\mu}) = 6\rho_h^2 M_c(\boldsymbol{\mu}). \tag{10.13}$$

Moreover, the error on the cost functional is bounded by

$$|\mathcal{J}_h(\boldsymbol{\mu}) - \mathcal{J}_N(\boldsymbol{\mu})| \le \Delta_N^{\mathcal{J}}(\boldsymbol{\mu}) + 6\rho_h^2 M_c(\boldsymbol{\mu})(\Delta_N(\boldsymbol{\mu}))^3. \tag{10.14}$$

Proof. In order to estimate the Lipschitz constant $K_h^N(\boldsymbol{\mu})$ it is sufficient to exploit the continuity of the trilinear form $c(\cdot,\cdot,\cdot;\boldsymbol{\mu})$ and the definition of $d(\cdot,\cdot,\cdot;\boldsymbol{\mu})$,

$$\begin{aligned}
|dG[U_1](\delta U, \widehat{U}; \boldsymbol{\mu}) - dG[U_2](\delta U, \widehat{U}; \boldsymbol{\mu})| &= |dG[U_1 - U_2](\delta U, \widehat{U}; \boldsymbol{\mu})| \\
&\le |d(\delta\mathbf{v} + \mathbf{R}(\delta\mathbf{u}), \mathbf{v}_1 - \mathbf{v}_2 + \mathbf{R}(\mathbf{u}_1) - \mathbf{R}(\mathbf{u}_2), \widehat{\boldsymbol{\lambda}}; \boldsymbol{\mu})| \\
&\quad + |d(\widehat{\mathbf{v}} + \mathbf{R}(\widehat{\mathbf{u}}), \delta\mathbf{v} + \mathbf{R}(\delta\mathbf{u}), \boldsymbol{\lambda}_1 - \boldsymbol{\lambda}_2; \boldsymbol{\mu})| \\
&\quad + |d(\widehat{\mathbf{v}} + \mathbf{R}(\widehat{\mathbf{u}}), \mathbf{v}_1 - \mathbf{v}_2 + \mathbf{R}(\mathbf{u}_1) - \mathbf{R}(\mathbf{u}_2), \delta\boldsymbol{\lambda}; \boldsymbol{\mu})| \\
&\le 6\rho_h^2 M_c(\boldsymbol{\mu})\, \|U_1 - U_2\|_{\mathcal{X}} \|\delta U\|_{\mathcal{X}} \|\widehat{U}\|_{\mathcal{X}},
\end{aligned}$$

so that $K_h^N(\boldsymbol{\mu}) = 6\rho^2 M_c(\boldsymbol{\mu})$ (which actually does not depend on N). In order to estimate the remainder term in (6.7), we first compute the second derivative of $G(\cdot,\cdot;\boldsymbol{\mu})$ at U,

$$d^2G[U](\widehat{U}, \widehat{U}, \widehat{U}; \boldsymbol{\mu}) = 3\, d(\widehat{\mathbf{v}} + \mathbf{R}(\widehat{\mathbf{u}}), \widehat{\mathbf{v}} + \mathbf{R}(\widehat{\mathbf{u}}), \widehat{\boldsymbol{\lambda}}; \boldsymbol{\mu}).$$

Then, by the continuity of $d(\cdot,\cdot,\cdot;\boldsymbol{\mu})$ we obtain

$$|\mathcal{R}(E_N(\boldsymbol{\mu});\boldsymbol{\mu})| \leq \sup_{W\in[U_N,U_h]} |d^2G[W](E_N(\boldsymbol{\mu}),E_N(\boldsymbol{\mu}),E_N(\boldsymbol{\mu});\boldsymbol{\mu})| \leq 6\rho_h^2 M_c(\boldsymbol{\mu})\|E_N(\boldsymbol{\mu})\|_{\mathcal{X}}^3,$$

and (10.14) easily follows. □

11. Application to a bypass graft design problem. Bypass grafting is a surgical procedure to create an alternate channel for blood flow, bypassing an obstructed or damaged portion of a vessel. However, it is well known (see, e.g., [46]) that arterial bypass grafts tend to fail after some years due to restenosis formation. Therefore, the design of bypass grafts seeks to minimize suitable haemodynamics indicators of the restenosis risk, such as the wall shear stress or the vorticity downstream the anastomosis. The optimization process is typically performed with respect to some geometrical design variable like the anastomosis angle or the graft-to-host diameter ratio. As recently proposed in [39], we rather follow a different approach which is based on the solution of a suitable optimal boundary control problem, for which the control function is the Dirichlet boundary condition representing the flow entering into the artery from the graft on the boundary Γ_C (see Fig. 11.1). Thus, the geometrical properties of the bypass graft are synthesized into the velocity profile $\mathbf{u}$ imposed at the bypass anastomosis, so that the shape optimization problem is turned into an optimal control one.

We consider an idealized two-dimensional partially occluded artery as in Fig. 11.1. The optimal control problem reads: seek $(\mathbf{v},\pi,\mathbf{u})$ such that the cost functional[6]

$$\mathcal{J}(\mathbf{v},\mathbf{u};\boldsymbol{\mu}) = \frac{1}{2}\int_{\Omega_{\text{obs}}(\boldsymbol{\mu})} |\nabla\times\mathbf{v}|^2\,d\Omega + \frac{1}{2\mu_3}\int_{\Gamma_C(\boldsymbol{\mu})} |\nabla_\Gamma \mathbf{u}|^2 d\Gamma \tag{11.1}$$

is minimized subject to the steady Navier-Stokes equations (10.2) together with the following boundary conditions:

$$\begin{aligned} -\pi\mathbf{n}+\nu(\nabla\mathbf{v})\mathbf{n} &= \mathbf{0} && \text{on } \Gamma_N \\ \mathbf{v} &= \mathbf{0} && \text{on } \Gamma_w(\boldsymbol{\mu}) \\ \mathbf{v} &= \mathbf{g}_{\text{res}}(\boldsymbol{\mu}) && \text{on } \Gamma_D \\ \mathbf{v} &= \mathbf{u} && \text{on } \Gamma_C(\boldsymbol{\mu}). \end{aligned} \tag{11.2}$$

Moreover, in order to obtain a physically meaningful problem, we enforce the total conservation of fluxes by adding the following constraint on the control variable

$$\int_{\Gamma_C(\boldsymbol{\mu})} \mathbf{u}\cdot\mathbf{n}\,d\Gamma = C(\boldsymbol{\mu}) := C_T - \int_{\Gamma_D} \boldsymbol{g}_{\text{res}}(\mu_2)\,d\Gamma, \tag{11.3}$$

being $C_T = 1$ the physiological flow rate of the host artery.

We consider the following parameters: the inverse of the kinematic viscosity $\mu_1 = 1/\nu \in [40,100]$; the percentage $\mu_2 \in [0,40]$ of residual flow $\mathbf{g}_{\text{res}}(\mu_2) = 6\mu_2/100\, y(1-y)$ in the host artery; the penalization parameter $\mu_3 \in [0.05,10]$ in the cost functional; the length of the control boundary $\mu_4 \in [0.5,1.2]$ (modeling the graft diameter). To handle the geometric parametrization and provide an affine decomposition of the

[6]Here ∇_Γ denotes the surface gradient operator on $\Gamma_C(\boldsymbol{\mu})$, see e.g. [18].

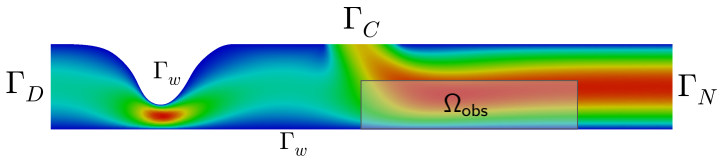

FIG. 11.1. *Domain and boundaries for the bypass problem.*

problem, we divide the domain $\Omega(\mu_4)$ into three subdomains Ω_1, $\Omega_2(\mu_4)$ and $\Omega_3(\mu_4)$, see Figure 11.1. Provided this decomposition of the domain, we can easily build an affine geometrical mapping such that, by tracing the problem back to the reference domain $\Omega = \Omega(\bar{\mu}_4)$ with $\bar{\mu}_4 = 0.8$, we obtain the affine decomposition (5.9)-(5.10) with $Q_d = 19$ and $Q_g = 28$.

For the finite element approximation, we use a mesh made of 30 926 triangular elements and 15 843 vertices, so that the total number of degrees of freedom is $N^h = 92\,239$; the dimension of the control space is $\dim(\mathcal{U}_h) = 104$.

11.1. Strong form of the optimality system. After integration by parts, it can be shown (see [9, 27] for similar problems) that system (10.11) constitutes the weak formulation for the coupled boundary value problem formed by the state equation (10.2)-(11.2), the adjoint equation

(11.4)
$$\begin{cases} -\dfrac{1}{\mu_1}\Delta\boldsymbol{\lambda} + (\nabla\mathbf{v})^T\boldsymbol{\lambda} - (\mathbf{v}\cdot\nabla)\boldsymbol{\lambda} + \nabla\eta = \chi_{obs}\nabla\times(\nabla\times\mathbf{v}) & \text{in } \Omega(\boldsymbol{\mu}) \\ \nabla\cdot\boldsymbol{\lambda} = 0 & \text{in } \Omega(\boldsymbol{\mu}) \\ -\eta\mathbf{n} + \nu(\nabla\boldsymbol{\lambda})\mathbf{n} + (\mathbf{v}\cdot\mathbf{n})\boldsymbol{\lambda} = \mathbf{0} & \text{on } \Gamma_N \\ \boldsymbol{\lambda} = \mathbf{0} & \text{on } \partial\Omega(\boldsymbol{\mu})\setminus\Gamma_N, \end{cases}$$

the optimality equation[7],

(11.5)
$$\begin{cases} -\mu_3\Delta_\Gamma\mathbf{u} + \kappa\mathbf{n} = \eta\mathbf{n} - \dfrac{1}{\mu_1}(\nabla\boldsymbol{\lambda})\mathbf{n} & \text{on } \Gamma_C(\boldsymbol{\mu}) \\ \mathbf{u} = \mathbf{0} & \text{on } \partial\Gamma_C(\boldsymbol{\mu}), \end{cases}$$

and the integral constraint (11.3) expressing the conservation of fluxes.

11.2. Assessment of the error estimates. As a first test case we consider as parameter only the inverse of the viscosity $\mu_1 \in [40, 100]$, fixing the others to[8] $\mu_2 = 30$, $\mu_3 = 1$, $\mu_4 = 0.8$. We first compute an approximation of the stability factor by constructing the interpolant surrogate: using the adaptive procedure detailed in [41], $\beta_I(\boldsymbol{\mu})$ is built by RBF interpolation of $\beta_h(\boldsymbol{\mu})$ computed in 5 interpolation points. Then, we run the greedy algorithm to construct the ROM, using $\Delta_N(\boldsymbol{\mu})$ as error estimate. Through this procedure, we select $N_{\max} = 12$ sample points with a fixed tolerance $\varepsilon_{tol} = 10^{-5}$ so that $\Delta_{N_{\max}}(\boldsymbol{\mu}) \le \varepsilon_{tol}\ \forall\boldsymbol{\mu} \in \Xi_{\text{train}}$, being Ξ_{train} a training set of 250 random points.

In Fig. 11.2 we compare, for $N = 1, \dots, N_{\max}$, the error bound $\Delta_N(\boldsymbol{\mu})$ with the true error between the full and reduced-order solutions: the estimate correctly reproduce the convergence of the error, however it shows a large effectivity $\eta_N(\boldsymbol{\mu})$

[7] We denote by Δ_Γ the Laplace-Beltrami operator on $\Gamma_C(\boldsymbol{\mu})$, see e.g. [18].
[8] In this case the affine decomposition reduces to $Q_g = 6$ and $Q_d = 3$ terms.

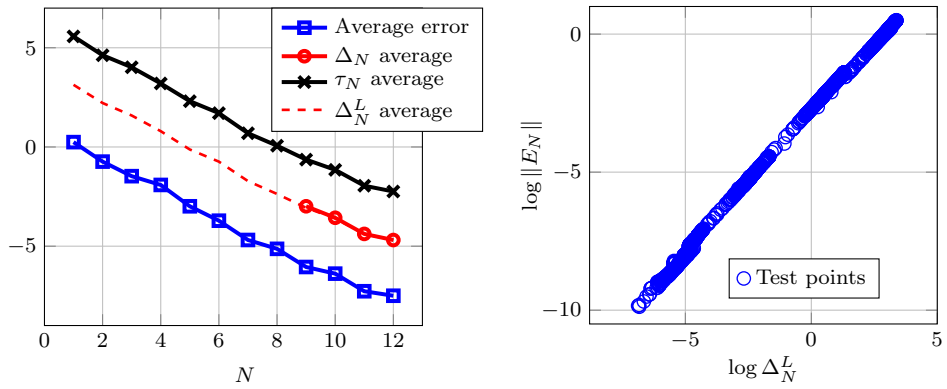

FIG. 11.2. *Bypass problem, 1 parameter case. On the left: average absolute error and estimate over a testing set of* 80 *random points in the parameter space (vertical axis in log scale). On the right: plot of the error* $\|E_N(\boldsymbol{\mu})\|_{\mathcal{X}}$ *versus the linear estimator* $\Delta_N^L(\boldsymbol{\mu})$ *(computed for* $N = 1, 4, 8$ *and* 80 *random parameter values).*

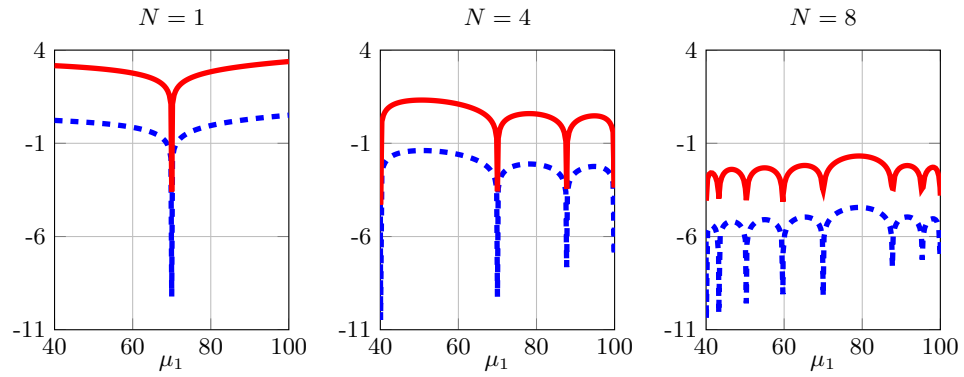

FIG. 11.3. *Bypass problem, 1 parameter case. Error* $\|E_N(\boldsymbol{\mu})\|_{\mathcal{X}}$ *(dashed blue line) and linear estimator* $\Delta_N^L(\boldsymbol{\mu})$ *(solid red line) for* $N = 1, 4, 8$ *as functions of* μ_1*.*

of order 10^3. Moreover, the proximity indicator $\tau_N(\boldsymbol{\mu})$ is smaller than one only for (on average) $N \geq 9$, so that the error bound $\Delta_N(\boldsymbol{\mu})$ is not available even when the true error is considerably small (for instance below 10^{-2}). In Fig. 11.2 we also report a pool of 240 test points $(\Delta_N^L(\boldsymbol{\mu}), \|E_N(\boldsymbol{\mu})\|)$ for different parameter values, while Fig. 11.3 shows the distributions of the error $\|E_N(\boldsymbol{\mu})\|_{\mathcal{X}}$ and the distribution of the linear estimator $\Delta_N^L(\boldsymbol{\mu})$ as functions of μ_1 for different values of N. It is rather evident the strong correlation of the error with $\Delta_N^L(\boldsymbol{\mu})$, which can therefore be used as a reliable error indicator in combination with the regression model described in Section 9.

Thus, considering the same setup, we now employ Algorithm 1 to build the reduced spaces. Thanks to the improved sharpness of the error indicator, the procedure selects only $N_{\max} = 7$ sample points to achieve a tolerance $\varepsilon_{tol} = 10^{-5}$ on the maximum error over Ξ_{train}. From a computational standpoint, we gain both in the offline phase, where 5 iterations of the greedy algorithm are avoided, and in the online phase, where a smaller system has to be solved. As a result, the solution of the reduced optimization problem takes less than 0.1 s, while the high-fidelity one requires on average

90 seconds to be solved[9].

In Fig. 11.4 we report the error behavior versus N, as well as its distribution in the parameter space for $N = 7$. The final regression model obtained at $N = 7$ is reported in Fig. 11.5 (left), where a set of 560 test points (generated from the convergence analysis of Fig. 11.4, left) is also shown. We observe that the regression model slightly underestimates the true error in the untrained region corresponding to $\Delta_N^L \in [10^{-4}, 10^{-1}]$. This is mainly due to the *reproductive* training points $\{(\Delta_n^L(\boldsymbol{\mu}^n), \|E_n(\boldsymbol{\mu}^n)\|)\}_{n=1}^7$, which distort the regression model at some extent. For this reason, we also report in Fig. 11.5 the regression model built upon the following set of $M_r = N(N-1)/2$ *predictive* training points

$$\mathcal{T}_N = \Big\{ \big(\Delta_n^L(\boldsymbol{\mu}^i),\, \|E_n(\boldsymbol{\mu}^i)\|_{\mathcal{X}}\big), \quad n = 1, \dots, i-1, \quad i = 1, \dots, N \Big\}. \tag{11.6}$$

Even though in this case it never underestimates the true error, the regression model is so poor in the untrained region $\Delta_N^L \lesssim 10^{-4}$ that it could possibly lead to the selection of snapshots that are already included during the greedy algorithm. Therefore, we recommend the use of the training set (9.5).

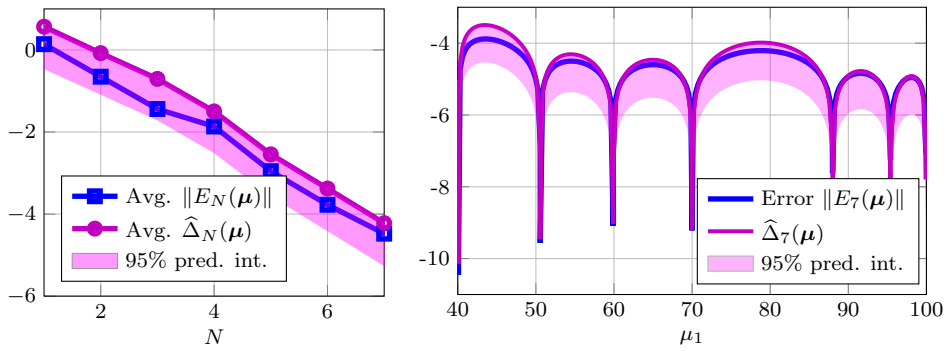

FIG. 11.4. *Bypass problem, 1 parameter case. On the left: average (over a testing set of 80 random points in the parameter space) absolute error* $\|E_N(\boldsymbol{\mu})\|$ *and error indicator* $\widehat{\Delta}_N(\boldsymbol{\mu})$ *for* $N = 1, \dots, 7$ *(vertical axis in log scale). On the right: error and error indicator for* $N = 7$ *as functions of* μ_1.

11.3. Parameter space exploration. We now let all the four parameters free to vary in $\mathcal{D}$. Due to the extent of the parameter space and the high number of terms in the affine decomposition, in this case we adopt a POD-based approach to build the ROM. We start by constructing the interpolant $\beta_I(\boldsymbol{\mu})$ of the stability factor by computing $\beta_h(\boldsymbol{\mu})$ in 40 interpolation points. Then, we solve the full-order model in correspondence of $N_s = 200$ parameter values selected by LHS sampling. We build the reduced spaces following the procedure detailed in Section 10.4 retaining $N = 45$ POD modes; the singular values of the snapshots matrix are shown in Fig. 11.6. Once the ROM is built, we compute the ingredients required for the evaluation of the dual norm of the residual. Finally, we generate the regression model (9.4) using as training points a random subset of $\mathcal{T}_N$ (as defined in (9.6)) of dimension 200. This

[9]The research code used in this work has been developed in the MATLAB® environment. For the bypass problem all the full-order linear systems are solved in one-shot using the sparse direct solver provided by MATLAB. Offline computations are performed on a node (with two Intel Xeon E5-2660 processors and 64 GB of RAM) of the SuperB cluster at EPFL. Online computations are performed on a workstation with a Intel Core i5-2400S processor and 16 GB of RAM.

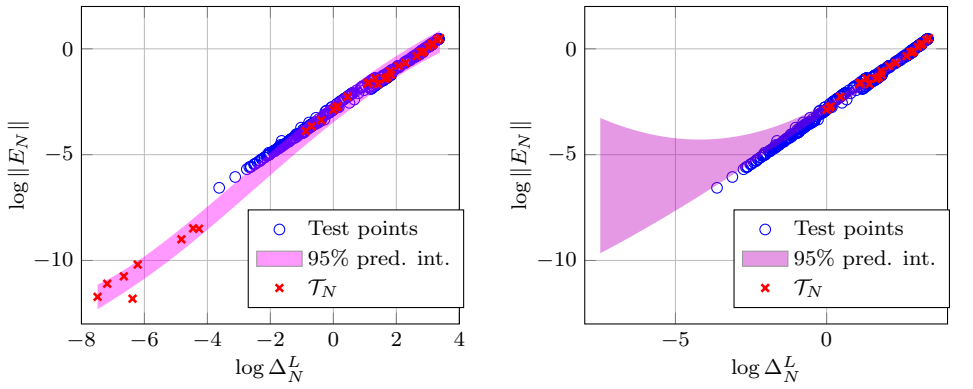

FIG. 11.5. *Bypass problem, 1 parameter case. Comparison between the* 95% *prediction intervals obtained using* $\mathcal{T}_N$ *as defined in* (9.5) *(on the left) and the one defined in* (11.6) *(on the right). In both cases, the set of test points is the one generated from the the convergence analysis of Fig. 11.4 (left plot).*

latter and the resulting regression model are shown in Fig. 11.7, where we also report the convergence with respect to N of $\|E_N(\boldsymbol{\mu})\|_{\mathcal{X}}$ and $\widehat{\Delta}_N(\boldsymbol{\mu})$. In Fig. 11.8 we show the optimal state velocity obtained by solving the reduced optimization problem for different values of the parameters.

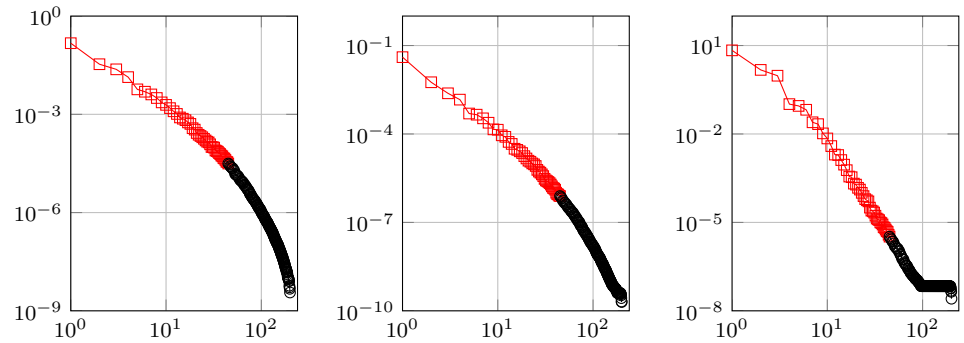

(a) state velocity (b) state pressure (c) control

FIG. 11.6. *Bypass problem, 4 parameters case. Decay of the singular values (denoted by* σ*) of the state velocity, state pressure and control snapshot matrices. Red squares correspond to the retained modes, while black circles correspond to the discarded ones.*

As regards the computational aspects, we notice a significant degradation of the online performances with respect to the previous case: the solution of the reduced optimization problem now takes on average 3 seconds. This is mainly due to the cost of assembling the reduced Jacobian matrix at each Newton iteration. Indeed, the assembly of $d\mathbf{G}_N(\cdot;\boldsymbol{\mu})$ requires to perform $5NQ_c$ additions of dense, square matrices of dimension $9N+1$, yielding a computational complexity of $\mathcal{O}(Q_c N^3)$. As a result, at each Newton iteration, the 95% of the time is spent assembling the reduced operator, and only the remaining 5% solving the linear system. A first remedy to this computational bottleneck would be to exploit a suitable parallel implementation of the operator assembly. On top of this, a more intrusive approach would rely on the use of local reduced bases (see e.g. [23, 2]) in order to lower the N^3 leading term in the operations count.

As a matter of fact however, even relying on an inefficient implementation, the reduced model provides a speedup of at least one order of magnitude, which is expected to further increase as the size and complexity of the underlying full-order model increase.

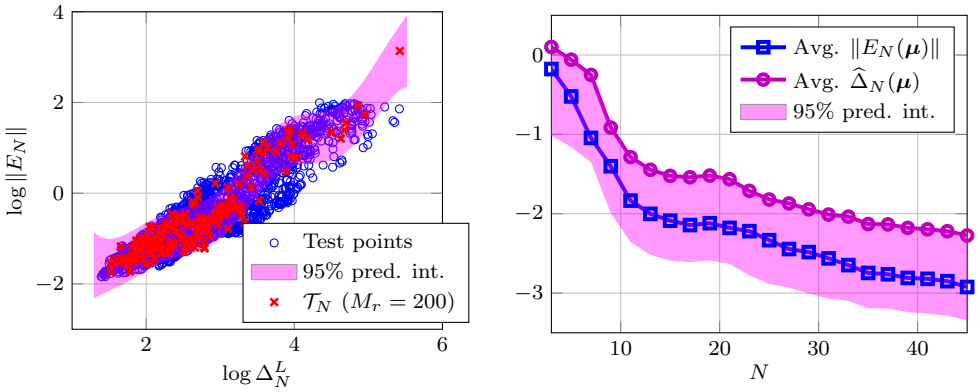

FIG. 11.7. *Bypass problem, 4 parameters case. On the left: training set $\mathcal{T}_N$, 95% predictive intervals and test points. On the right: convergence of the relative error and error indicator averaged on a test sample of 150 random parameter values.*

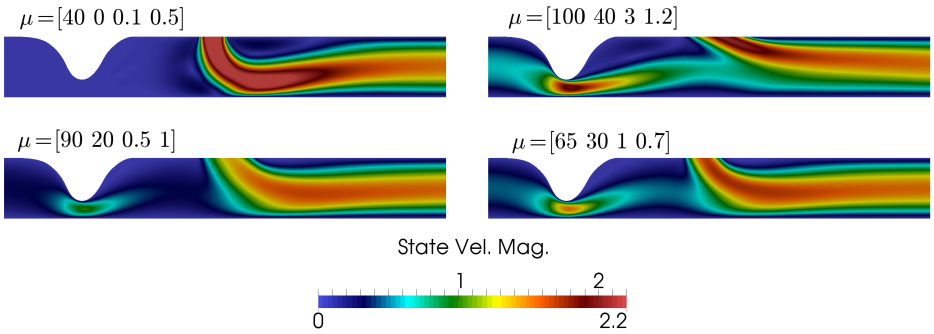

FIG. 11.8. *Bypass problem. Optimal state velocity obtained by solving the ROM for different values of $\boldsymbol{\mu}$.*

12. Vorticity minimization around a bluff body. In this section, we deal with a problem of vorticity minimization through suction/injection of fluid on the downstream portion of a bluff body, see e.g. [24, 16, 44]. In particular, we consider a body embedded in a three-dimensional viscous flow modeled by the steady incompressible Navier-Stokes equations. The goal consists in minimizing the viscous energy dissipation in the wake of the body, by regulating the flow across a portion of its boundary Γ_C. We minimize the following cost functional,

$$\mathcal{J}(\mathbf{v}, u; \boldsymbol{\mu}) = \frac{1}{2} \int_{\Omega_{\text{obs}}(\mu_1)} |\nabla \mathbf{v}|^2 \, d\Omega + \frac{1}{2\mu_3} \int_{\Gamma_C(\mu_1)} \left|\nabla_\Gamma u\right|^2 d\Gamma, \tag{12.1}$$

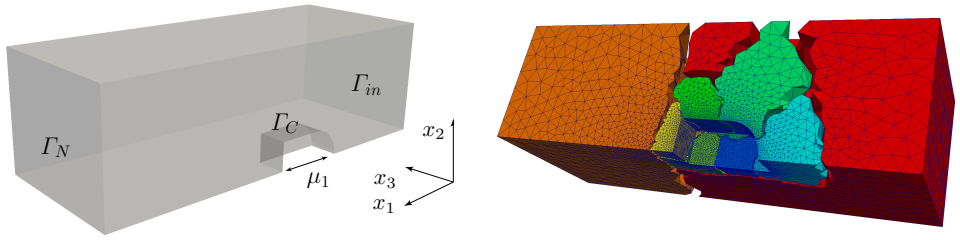

FIG. 12.1. *On the left: domain and boundaries for problem* (12.1)-(12.2). *On the body boundary we impose a no-slip condition except that on the control region; on the top, bottom and lateral boundaries of the domain we impose symmetry conditions. On the right: computational mesh and its decomposition into 8 subdomains used for the preconditioner* (12.3).

subject to the steady Navier-Stokes equations (10.2) together with the following boundary conditions:

$$
\begin{aligned}
\mathbf{v}\cdot\mathbf{t}=0,\ \mathbf{v}\cdot\mathbf{n}=u \quad & \text{on } \Gamma_C(\mu_1)\\
\mathbf{v}=\mu_2\mathbf{t} \quad & \text{on } \Gamma_{in}\\
\mathbf{v}=\mathbf{0} \quad & \text{on } \Gamma_w\\
\mathbf{v}\cdot\mathbf{n}=\mathbf{0},\ (\nabla\mathbf{v})\mathbf{n}\cdot\mathbf{t}=\mathbf{0} \quad & \text{on } \Gamma_s(\mu_1)\\
-\pi\mathbf{n}+\nu(\nabla\mathbf{v})\mathbf{n}=\mathbf{0} \quad & \text{on } \Gamma_N,
\end{aligned}
\tag{12.2}
$$

where $\mathbf{n}$ and $\mathbf{t}$ are the outward normal and tangential unit vectors to the boundary. We impose an horizontal constant velocity profile on the inflow boundary Γ_{in}, no-slip conditions on Γ_w, symmetry conditions on Γ_s, no-stress conditions on Γ_N and Dirichlet conditions on the control boundary Γ_C. In particular, we consider suction/injection of fluid through the control boundary only in the normal direction, while we impose a no-slip condition in the tangential one. See Fig. 12.1 for the details of the geometry.

The parameters are given by: the length $\mu_1 \in [0.1, 0.3]$ of the control boundary, the magnitude $\mu_2 \in [0.5, 3]$ of the inflow velocity profile and the inverse of the penalization factor $\mu_3 \in [1, 800]$. The kinematic viscosity ν is fixed to 0.03. We employ a decomposition of the geometry into three subdomains to obtain an affine decomposition with $Q_g = 27$ and $Q_d = 18$.

12.1. High-fidelity solver. Using a mesh made of 92 280 tetrahedral elements and 17 478 vertices, the total number of degrees of freedom is $N^h = 140\,441$; in particular, the dimension of the control space is $\dim(\mathcal{U}_h) = 617$. For any given $\boldsymbol{\mu}$, we solve the resulting nonlinear system employing the full-space Newton-Krylov-Schwarz solver proposed in [48], i.e. we use the GMRES method with a two-level Additive Schwarz (AS) preconditioner to solve the linear system arising at each Newton step (4.7). To build the AS preconditioner for the Hessian matrix $\mathrm{K} = d\mathbf{G}(\cdot;\cdot)$, we first partition the domain Ω into overlapping subdomains Ω_i^δ, $i = 1\ldots, M$, featuring an overlap of size $\delta = h$ (see Fig. 12.1 on the right). We then build suitable restriction matrices $\mathrm{R}_i \in \mathbb{R}^{N_m^h \times N^h}$ so that the local matrices $\mathrm{K}_m = \mathrm{R}_m \mathrm{K} \mathrm{R}_m^T \in \mathbb{R}^{N_m^h \times N_m^h}$ correspond to the restriction of K to the subdomains Ω_m^δ. Finally we build a suitable coarse correction matrix $\mathrm{K}_0 = \mathrm{R}_0 \mathrm{K} \mathrm{R}_0^T \in \mathbb{R}^{n_v M \times n_v M}$ (n_v being the number of variables), whose restriction matrix $\mathrm{R}_0 \in \mathbb{R}^{n_v M \times N^h}$ is obtained by aggregation [52]. The

AS preconditioner is then defined as

$$\mathrm{P}_{AS}^{-1} = \sum_{m=0}^{M} \mathrm{R}_m^T \mathrm{K}_m^{-1} \mathrm{R}_m, \tag{12.3}$$

K_m^{-1} being the inverse of K_m, here computed by means of an exact LU factorization; each local preconditioner is then applied in parallel.

Using 8 subdomains, the GMRES method converges on average in 50 iterations up to a tolerance of 10^{-8} on the relative norm of the residual. The outer Newton loop takes on average 7 iterations to reach a tolerance of 10^{-7} on the relative norm of the increment. Overall, solving the full-order problem for a given $\boldsymbol{\mu} \in \mathcal{D}$ takes about 5 minutes.

12.2. Reduced-order approximation. We adopt a POD-based approach to build the ROM: we solve the full-order model in correspondence of $N_s = 100$ parameter values selected by LHS sampling and then retain $N = 30$ POD modes. Once the ROM is built, we compute the ingredients required for the evaluation of the dual norm of the residual. Finally, we build the regression model (9.4) using as training points a random subset of $\mathcal{T}_N$ (as defined in (9.6)) of dimension 200. This latter and the resulting regression model are shown in Fig. 12.2, where we also report the convergence of $\|E_N(\boldsymbol{\mu})\|_{\mathcal{X}}$ and $\widehat{\Delta}_N(\boldsymbol{\mu})$ with respect to N.

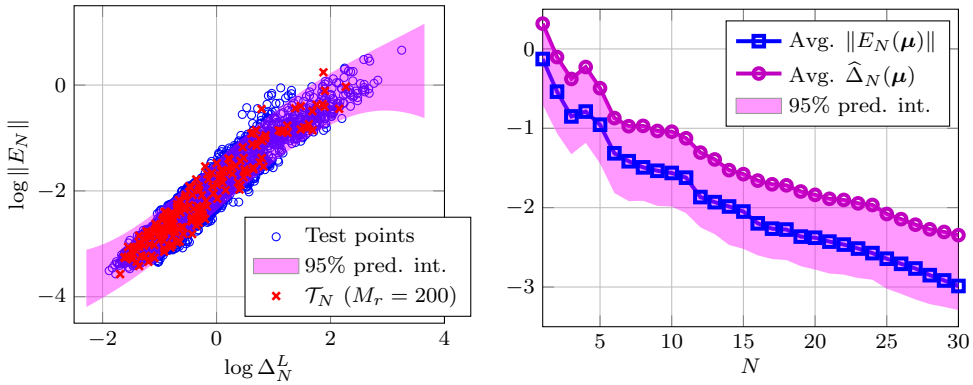

FIG. 12.2. *Bluff body problem. On the left: training set $\mathcal{T}_N$, 95% predictive intervals and test points. On the right: convergence of the relative error and error indicator averaged on a test sample of 100 random parameter values.*

Figure 12.3 shows the streamlines of the optimal state velocity around the body obtained by solving the reduced optimization problem for $\boldsymbol{\mu} = (0.15, 3, 1)$ and $\boldsymbol{\mu} = (0.15, 3, 800)$. The benefits of the optimization in reducing the vorticity are clearly visible, as the small vortices occurring for $\mu_3 = 1$ (which yields an almost uncontrolled velocity field) disappears for $\mu_3 = 800$. Moreover, solving the reduced problem takes only 2 seconds, leading to a speedup of about 150.

13. Conclusions. In this work, we developed a general model reduction framework for the solution of parametrized quadratic optimization problems governed by nonlinear PDEs. By adopting a *full space* (or *all-at-once*) formulation, the ROM was generated through a Galerkin projection of the high-fidelity optimality system onto a low-dimensional space. It was demonstrated how a simultaneous reduction of the state, control and adjoint spaces can be achieved employing a Reduced Basis greedy approach as well as Proper Orthogonal Decomposition.

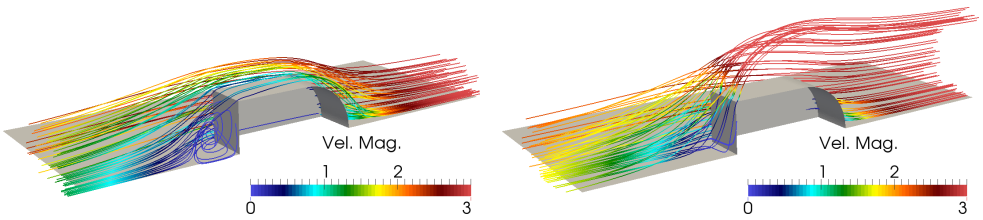

FIG. 12.3. *Streamlines of the optimal state velocity around the bluff body obtained by solving the ROM for* $\boldsymbol{\mu} = (0.15, 3, 1)$ *(left) and* $\boldsymbol{\mu} = (0.15, 3, 800)$ *(right).*

In both cases, the availability of a tight error estimate is crucial to bound the offline computational costs and effectively quantify the accuracy of the reduced approximation in the online phase. To this end, we first derived a rigorous – yet too pessimistic in practice – error bound, which was then used to generate a much tighter error indicator.

The entire procedure was equipped with a suitable offline-online computational strategy, ensuring the efficiency of the online computations. As a result, our numerical tests on two different boundary control problems constrained by the Navier-Stokes equations showed that significant speedups can be achieved, still ensuring a good accuracy.

Acknowledgments. I would like to thank Dr. L. Dedè, Dr. A. Manzoni, Prof. A. Quarteroni and Prof. G. Rozza for the helpful discussions and suggestions.

REFERENCES

[1] V. AKCELIK, G. BIROS, O. GHATTAS, J. HILL, D. KEYES, AND B. WAANDERS, *Parallel Algorithms for PDE-Constrained Optimization*, in Parallel Processing for Scientific Computing, M.A. Heroux, P. Raghavan, and H.D. Simon, eds., Philadephia, PA, 2006, SIAM.

[2] D. AMSALLEM AND C. FARHAT, *An online method for interpolating linear parametric reduced-order models*, SIAM J. Sci. Comput., 33 (2011), p. 2169.

[3] D. AMSALLEM, M.J. ZAHR, Y. CHOI, AND C. FARHAT, *Design optimization using hyper-reduced-order models*, Struct. Multidiscip. O., (2014), pp. 1–22.

[4] E. ARIAN, M. FAHL, AND E.W. SACHS, *Trust-region proper orthogonal decomposition for flow control*, Tech. Report Tech. report ICASE 2000-25, Institute for Computer Applications in Science and Engineering, Langley, VA, 2000.

[5] M. BARRAULT, Y. MADAY, N. NGUYEN CUONG, AND A.T. PATERA, *An 'empirical interpolation' method: application to efficient reduced-basis discretization of partial differential equations*, C. R. Acad. Sci. Paris. Sér. I Math., 339 (2004), pp. 667 – 672.

[6] R. BECKER, H. KAPP, AND R. RANNACHER, *Adaptive Finite Element Methods for Optimal Control of Partial Differential Equations: Basic Concept*, SIAM J. Control Optim., 39 (2000), pp. 113–132.

[7] P. BENNER, E. SACHS, AND S. VOLKWEIN, *Model Order Reduction for PDE Constrained Optimization*, in Trends in PDE Constrained Optimization, G. Leugering, P. Benner, S. Engell, A. Griewank, H. Harbrecht, M. Hinze, R. Rannacher, and S. Ulbrich, eds., vol. 165 of International Series of Numerical Mathematics, Springer International Publishing, 2014, pp. 303–326.

[8] M. BERGMANN AND L. CORDIER, *Optimal control of the cylinder wake in the laminar regime by trust-region methods and POD reduced-order models*, J. Comput. Phys., 227 (2008), pp. 7813–7840.

[9] G. BIROS AND O. GHATTAS, *Parallel Lagrange–Newton–Krylov–Schur Methods for PDE-Constrained Optimization. Part II: The Lagrange–Newton Solver and Its Application to Optimal Control of Steady Viscous Flows*, SIAM J. Sci. Comput., 27 (2005), pp. 714–739.

[10] P. BOCHEV, C. DOHRMANN, AND M. GUNZBURGER, *Stabilization of low-order mixed finite elements for the Stokes equations*, SIAM J. Numer. Anal., 44 (2006), pp. 82–101.

[11] F. BREZZI, J. RAPPAZ, AND P.A. RAVIART, *Finite dimensional approximation of nonlinear problems. Part I: Branches of nonsingular solutions*, Numer. Math., 36 (1980), pp. 1–25.

[12] G. Caloz and J. Rappaz, *Numerical analysis for nonlinear and bifurcation problems*, in Handbook of Numerical Analysis, Vol. V, P.G. Ciarlet and J.L. Lions, eds., Techniques of Scientific Computing (Part 2), Elsevier Science B.V., 1997, pp. 487–637.

[13] K. Carlberg, C. Farhat, J. Cortial, and D. Amsallem, *The GNAT method for nonlinear model reduction: Effective implementation and application to computational fluid dynamics and turbulent flows*, J. Comput. Phys., 242 (2013), pp. 623 – 647.

[14] S. Chaturantabut and D.C. Sorensen, *Nonlinear model reduction via discrete empirical interpolation*, SIAM J. Sci. Comput., 32 (2010), pp. 2737–2764.

[15] S.S. Collis and M. Heinkenschloss, *Analysis of the streamline upwind/Petrov Galerkin method applied to the solution of optimal control problems.* tech. Report CAAM TR02-01, Rice University, March 2012.

[16] L. Dedè, *Optimal flow control for Navier-Stokes equations: Drag minimization*, Internat. J. Numer. Methods Fluids, 55 (2007), pp. 347 – 366.

[17] L. Dedè, *Reduced basis method and a posteriori error estimation for parametrized linear-quadratic optimal control problems*, SIAM J. Sci. Comput., 32 (2010), pp. 997–1019.

[18] M.C. Delfour and J.-P. Zolésio, *Shapes and geometries: metrics, analysis, differential calculus, and optimization*, vol. 22, SIAM, Philadelphia, PA, 2011.

[19] M. Desai and K. Ito, *Optimal controls of Navier-Stokes equations*, SIAM J. Control Optim., 32 (1994), pp. 1428–1446.

[20] M. Dihlmann and B. Haasdonk, *Certified Nonlinear Parameter Optimization with Reduced Basis Surrogate Models*, Proc. Appl. Math. Mech, 13 (2013), pp. 3–6.

[21] M. Drohmann and K. Carlberg, *The ROMES Method for Statistical Modeling of Reduced-Order-Model Error*, SIAM/ASA Journal on Uncertainty Quantification, 3 (2015), pp. 116–145.

[22] M. Drohmann, B. Haasdonk, and M. Ohlberger, *Reduced basis approximation for nonlinear parametrized evolution equations based on empirical operator interpolation*, SIAM J. Sci. Comput., 34 (2012), pp. A937–A969.

[23] J. Eftang, A. Patera, and E. Rønquist, *An* hp *certified reduced basis method for parametrized elliptic partial differential equations*, SIAM J. Sci. Comput., 32 (2010), pp. 3170–3200.

[24] O. Ghattas and J.-H. Bark, *Optimal control of two-and three-dimensional incompressible Navier–Stokes flows*, J. Comput. Phys., 136 (1997), pp. 231–244.

[25] V. Girault and P.-A. Raviart, *Finite element methods for Navier-Stokes equations: Theory and algorithms*, Springer-Verlag, Berlin and New York, 1986.

[26] M.D. Gunzburger, *Perspectives in flow control and optimization*, SIAM, Philadelphia, 2003.

[27] M.D. Gunzburger, L. S. Hou, and Th. P. Svobodny, *Analysis and finite element approximation of optimal control problems for the stationary Navier-Stokes equations with Dirichlet controls*, ESAIM: Math. Model. Numer. Anal., 25 (1991), pp. 711–748.

[28] M. Heinkenschloss, *Formulation and Analysis of a Sequential Quadratic Programming Method for the Optimal Dirichlet Boundary Control of Navier-Stokes Flow*, in in Optimal Control, Theory, Algorithms, and Applications. Kluwer Academic Publishers B.V, Kluwer Academic Publishers B.V, 1998, pp. 178–203.

[29] M. Hinze, R. Pinnau, M. Ulbrich, and S. Ulbrich, *Optimization with PDE constraints*, Springer, 2009.

[30] M. Hinze and S. Volkwein, *Proper orthogonal decomposition surrogate models for nonlinear dynamical systems: Error estimates and suboptimal control*, in Dimension Reduction of Large-Scale Systems, P. Benner, D.C. Sorensen, and V. Mehrmann, eds., vol. 45 of Lecture Notes in Computational Science and Engineering, Springer Berlin Heidelberg, 2005, pp. 261–306.

[31] P. Holmes, J. Lumley, and G. Berkooz, *Turbulence, coherent structures, dynamical systems and symmetry*, Cambridge University Press, UK, 1996.

[32] L. S. Hou and S. S. Ravindran, *Numerical approximation of optimal flow control problems by a penalty method: Error estimates and numerical results*, SIAM J. Sci. Comput., 20 (1999), pp. 1753–1777.

[33] K. Ito and K. Kunisch, *Lagrange Multiplier Approach to Variational Problems and Applications*, Adv. Des. Control, SIAM, 2008.

[34] K. Ito and S. S. Ravindran, *A reduced basis method for control problems governed by PDEs*, Internat. Ser. Numer. Math., 126 (1998), pp. 153–168.

[35] M. Kahlbacher and S. Volkwein, *POD a-posteriori error based inexact SQP method for bilinear elliptic optimal control problems*, ESAIM: Math. Model. Numer. Anal., 46 (2012), pp. 491–511.

[36] M. Kärcher and M.A. Grepl, *A Certified Reduced Basis Method for Parametrized Elliptic Optimal Control Problems*, ESAIM Control Optim. Calc. Var., 20 (2014), pp. 416–441.

[37] M. Kärcher and M.A. Grepl, *A Posteriori Error Estimation for Reduced Order Solutions of Parametrized Parabolic Optimal Control Problems*, ESAIM: M2AN, 48 (2014), pp. 1615–1638.

[38] K. Kunisch and S. Volkwein, *Proper orthogonal decomposition for optimality systems*, ESAIM Math. Model. Numer. Anal., 42 (2008), pp. 1–23.

[39] T. Lassila, A. Manzoni, A. Quarteroni, and G. Rozza, *Boundary control and shape optimization for the robust design of bypass anastomoses under uncertainty*, ESAIM Math. Model. Numer. Anal., 47 (2013), pp. 1107–1131.

[40] A. Manzoni, *An efficient computational framework for reduced basis approximation and a posteriori error estimation of parametrized Navier-Stokes flows*, ESAIM: Math. Model. Numer. Anal., 48 (2014), pp. 1199–1226.

[41] A. Manzoni and F. Negri, *Heuristic strategies for the approximation of stability factors in quadratically nonlinear parametrized PDEs*, Advances in Computational Mathematics, (2015), pp. 1–34.

[42] A. Manzoni, S. Pagani, and T. Lassila, *Accurate solution of Bayesian inverse uncertainty quantification problems using model and error reduction methods*. MATHICSE Report Nr. 47.2014 (submitted), 2014.

[43] A. Manzoni, A. Quarteroni, and G. Rozza, *Shape optimization for viscous flows by reduced basis methods and free-form deformation*, Int. J. Numer. Meth. Fluids, 70 (2012), pp. 646–670.

[44] F. Negri, A. Manzoni, and G. Rozza, *Reduced basis approximation of parametrized optimal flow control problems for the Stokes equations*, Comput. Math. Appl., 69 (2015), pp. 319 – 336.

[45] F. Negri, G. Rozza, A. Manzoni, and A. Quarteroni, *Reduced Basis Method for Parametrized Elliptic Optimal Control Problems*, SIAM J. Sci. Comput., 35 (2013), pp. A2316–A2340.

[46] A.A. Owida, H. Do, and Y.S Morsi, *Numerical analysis of coronary artery bypass grafts: An over view*, Comput. Meth. Prog. Bio., 108 (2012), pp. 689 – 705.

[47] A. Paul-Dubois-Taine and D. Amsallem, *An adaptive and efficient greedy procedure for the optimal training of parametric reduced-order models*, Internat. J. Numer. Methods Engrg., (2014), pp. 1–31.

[48] E.E. Prudencio, R Byrd, and X.-C. Cai, *Parallel Full Space SQP Lagrange–Newton–Krylov–Schwarz Algorithms for PDE-Constrained Optimization Problems*, SIAM J. Sci. Comput., 27 (2006), pp. 1305–1328.

[49] C. Prud'homme, D.V. Rovas, K. Veroy, L. Machiels, Y. Maday, A.T. Patera, and G. Turinici, *Reliable real-time solution of parametrized partial differential equations: Reduced-basis output bound methods*, J. Fluid Eng., 124 (2002), pp. 70–80.

[50] C. E. Rasmussen and C. K. I. Williams, *Gaussian Processes for Machine Learning*, MIT Press, Cambridge, MA, 2006.

[51] G. Rozza, D.B.P. Huynh, and A.T. Patera, *Reduced basis approximation and a posteriori error estimation for affinely parametrized elliptic coercive partial differential equations*, Arch. Comput. Methods Engrg., 15 (2008), pp. 229–275.

[52] M. Sala, *Analysis of two-level domain decomposition preconditioners based on aggregation*, ESAIM: Math. Model. Numer. Anal., 38 (2004), pp. 765–780.

[53] L. Sirovich, *Turbulence and the dynamics of coherent structures, part i: Coherent structures*, Quart. Appl. Math., 45 (1987), pp. 561–571.

[54] R. Stefanescu, A. Sandu, and I.M. Navon, *POD/DEIM strategies for reduced data assimilation systems*. Computer Science Technical Report 3/2014, 2014.

[55] R. Temam, *Navier-Stokes Equations*, AMS Chelsea, Providence, Rhode Island, 2001.

[56] T. Tonn, K. Urban, and S. Volkwein, *Comparison of the reduced-basis and POD a-posteriori estimators for an elliptic linear-quadratic optimal control problem*, Math. Comput. Model. Dyn. Syst., 17 (2011), pp. 355–369.

[57] F. Tröltzsch and S. Volkwein, *POD a-posteriori error estimates for linear-quadratic optimal control problems*, Comput. Optim. Appl., 44 (2009), pp. 83–115.

[58] K. Veroy and A.T. Patera, *Certified real-time solution of the parametrized steady incompressible NavierStokes equations: rigorous reduced-basis a posteriori error bounds*, Int. J. Numer. Meth. Fl., 47 (2005), pp. 773–788.

[59] M.J. Zahr and C. Farhat, *Progressive construction of a parametric reduced-order model for PDE-constrained optimization*, Int. J. Numer. Meth. Eng., 102 (2015), pp. 1111–1135.

[60] E. Zeidler, *Nonlinear Functional Analysis and its Applications*, vol. I: Fixed-Point Theorems, Springer-Verlag, 1985.

Recent publications:

MATHEMATICS INSTITUTE OF COMPUTATIONAL SCIENCE AND ENGINEERING
Section of Mathematics
Ecole Polytechnique Fédérale
CH-1015 Lausanne

48.2014 MARCO PICASSO:
From the free surface flow of a viscoelastic fluid towards the elastic deformation of a solid

49.2014 FABIO NOBILE, FRANCESCO TESEI:
A multi level Monte Carlo method with control variate for elliptic PDEs with log-normal coefficients

***

01.2015 PENG CHEN, ALFIO QUARTERONI, GIANLUIGI ROZZA:
Reduced order methods for uncertainty quantification problems

02.2015 FEDERICO NEGRI, ANDREA MANZONI, DAVID AMSALLEM:
Efficient model reduction of parametrized systems by matrix discrete empirical interpolation

03.2015 GIOVANNI MIGLIORATI, FABIO NOBILE, RAÚL TEMPONE:
Convergence estimate in probability and in expectation for discrete least squares with noisy evaluations at random points

04.2015 FABIO NOBILE, LORENZO TAMELLINI, FRANCESCO TESEI, RAÚL TEMPONE:
An adaptive sparse grid alorithm for elliptic PDEs with lognormal diffusion coefficent

05.2015 MICHAEL STEINLECHNER:
Riemannian optimization for high-dimensional tensor completion

06.2015 V. R. KOSTIĆ, A. MIEDLAR, LJ. CVETKOVIĆ:
An algorithm for computing minimal Geršgorin sets

07.2015 ANDREA BARTEZZAGHI, LUCA DEDÈ, ALFIO QUARTERONI:
Isogeometric analysis of high order partial differential equations on surfaces

08.2015 IVAN FUMAGALLI, ANDREA MANZONI, NICOLA PAROLINI, MARCO VERANI:
Reduced basis approximation and a posteriori error estimates for parametrized elliptic eigenvalue problems

09.2015 DAVIDE FORTI, LUCA DEDÈ:
Semi-implicit BDF time discretization of the Navier-Stokes equations with VMS-LES modeling in a High Performance Computing framework

10.2015 PETAR SIRKOVIĆ, DANIEL KRESSNER:
Subspace acceleration for large-scale parameter-dependent Hermitian eigenproblems

11.2015 FEDERICO NEGRI:
A model order reduction framework for parametrized nonlinear PDE-constrained optimization